Published for SISSA by Springer

Received: August 1, 2022
Accepted: November 6, 2022
Published: July 6, 2023

Measurement of inclusive and differential cross sections for single top quark production in association with a W boson in proton-proton collisions at $\sqrt{s} = 13$ TeV

The CMS collaboration

E-mail: cms-publication-committee-chair@cern.ch

Abstract: Measurements of the inclusive and normalised differential cross sections are presented for the production of single top quarks in association with a W boson in proton-proton collisions at a centre-of-mass energy of 13 TeV. The data used were recorded with the CMS detector at the LHC during 2016–2018, and correspond to an integrated luminosity of 138 fb^{-1}. Events containing one electron and one muon in the final state are analysed. For the inclusive measurement, a multivariate discriminant, exploiting the kinematic properties of the events is used to separate the signal from the dominant $\mathrm{t\bar{t}}$ background. A cross section of $79.2 \pm 0.9\,(\mathrm{stat})\,^{+7.7}_{-8.0}\,(\mathrm{syst}) \pm 1.2\,(\mathrm{lumi})$ pb is obtained, consistent with the predictions of the standard model. For the differential measurements, a fiducial region is defined according to the detector acceptance, and the requirement of exactly one jet coming from the fragmentation of a bottom quark. The resulting distributions are unfolded to particle level and agree with the predictions at next-to-leading order in perturbative quantum chromodynamics.

Keywords: Hadron-Hadron Scattering, Top Physics

ArXiv ePrint: 2208.00924

https://doi.org/10.1007/JHEP07(2023)046

JHEP07(2023)046

Contents

1 Introduction

The electroweak production of single top quarks was first observed by the D0 [1] and CDF [2] Collaborations at the Fermilab Tevatron. At leading order, single top quark production proceeds mainly via three processes: the t-channel exchange of a virtual W boson, s-channel production, and the associated production of a top quark and a W boson (tW). The last channel, which was negligible at the Tevatron, represents a significant contribution to single top quark production at the CERN LHC. It is a very interesting production mechanism because of its interference with top quark pair ($\mathrm{t\bar{t}}$) production [3–5], its sensitivity to beyond the standard model (SM) physics [6–11], and its role as a background in several other analyses.

The definition of tW production at next-to-leading order (NLO) in perturbative quantum chromodynamics (QCD) shares final states with $\mathrm{t\bar{t}}$ production [3–5]. The cross section for tW production has been computed at approximate next-to-NLO order (NNLO) in QCD. Assuming a top quark mass (m_{t}) of 172.5 GeV, the theoretical NNLO cross section for tW production in proton-proton (pp) collisions at $\sqrt{s} = 13\,\mathrm{TeV}$ is $\sigma_{\mathrm{tW}}^{\mathrm{SM}}$ =

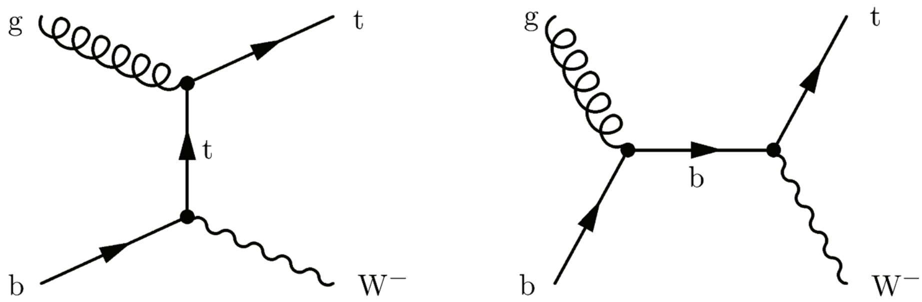

Figure 1. Leading-order Feynman diagrams for single top quark production in the tW mode. The charge-conjugate modes are implicitly included.

$71.7 \pm 1.8\,(\text{scale}) \pm 3.4\,(\text{PDF})$ pb [12], where the first uncertainty corresponds to the renormalisation (μ_R) and factorisation (μ_F) scale variations, and the second to using different parton distribution function (PDF) sets. The leading-order (LO) Feynman diagrams for tW production are shown in figure 1.

The tW channel was not accessible at the Tevatron due to its small cross section in $p\bar{p}$ collisions at $\sqrt{s} = 1.96$ TeV. At the LHC, however, evidence for this process in 7 TeV collision data was presented by ATLAS [13] and CMS [14]. At $\sqrt{s} = 8$ TeV, measurements by CMS [15] and ATLAS [16] were in good agreement with theoretical predictions.

At $\sqrt{s} = 13$ TeV the inclusive tW production cross section has been measured by both ATLAS [17] and CMS [18] using data recorded during 2016. Both measurements employed dileptonic ($e^{\pm}\mu^{\mp}$ for CMS and $e^{+}e^{-}$, $\mu^{+}\mu^{-}$, and $e^{\pm}\mu^{\mp}$ for ATLAS) channels. The measurement of the differential tW production cross section is particularly challenging due to the overwhelming background from $t\bar{t}$ events, with 80% [17] in the most tW-enriched category. The ATLAS experiment performed the first measurement of the tW production differential cross section [19], and a study [20] of the WWbb final state (that includes tW and $t\bar{t}$). Studies in the semileptonic channel have also been done recently at $\sqrt{s} = 13$ TeV by CMS [21] and at $\sqrt{s} = 8$ TeV by ATLAS [22].

This paper reports a measurement of inclusive and normalised differential tW production cross sections at $\sqrt{s} = 13$ TeV with dilepton final states ($e^{\pm}\mu^{\mp}$), using data collected with the CMS detector during 2016–2018, corresponding to an integrated luminosity of 138 fb^{-1}. The paper is structured as follows. A summary of the data and Monte Carlo (MC) samples used is provided in section 2. The object and event selection criteria are discussed in section 3. The signal extraction for the inclusive and differential measurements are detailed in sections 4 and 5, respectively. The systematic uncertainties are discussed in section 6. The inclusive and differential results are presented in section 7. Finally, a summary of both measurements is given in section 8. Tabulated results are provided in the HEPData record for this analysis [23].

2 The CMS detector and MC simulation

The central feature of the CMS apparatus is a superconducting solenoid of 6 m internal diameter, providing a magnetic field of 3.8 T. Within the solenoid volume are a silicon

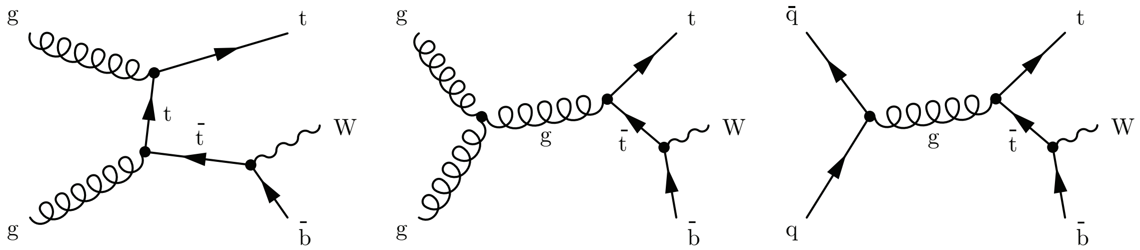

Figure 2. Feynman diagrams for tW single top quark production at NLO that are removed from the signal definition in the DR scheme. The charge-conjugate modes are implicitly included.

pixel and strip tracker, a lead tungstate crystal electromagnetic calorimeter, and a brass and scintillator hadron calorimeter, each composed of a barrel and two endcap sections. Forward calorimeters extend the pseudorapidity (η) coverage provided by the barrel and endcap detectors. Muons are detected in gas-ionisation chambers embedded in the steel flux-return yoke outside the solenoid. A more detailed description of the CMS detector, together with a definition of the coordinate system used and the relevant kinematic variables, can be found in ref. [24]. Events of interest are selected using a two-tiered trigger system. The first level (L1), composed of custom hardware processors, uses information from the calorimeters and muon detectors to select events at a rate of around 100 kHz within a fixed latency of about 4 μs [25]. The second level, known as the high-level trigger, consists of a farm of processors running a version of the full event reconstruction software optimized for fast processing, and reduces the event rate to around 1 kHz before data storage [26].

We rely on MC simulations to estimate the contributions from both signal and background processes. The tW signal samples are simulated at NLO in QCD using POWHEG v2 [27–29]. Two schemes are proposed to describe the tW signal: “diagram removal” (DR) [3], where all NLO diagrams that are doubly resonant (i.e. that can have two top quarks on-shell), such as those in figure 2, are excluded from the signal definition; and “diagram subtraction” (DS) [3, 30], in which the differential cross section is modified with a gauge-invariant subtraction term, which locally cancels the contribution of $\mathrm{t\bar{t}}$ diagrams. The DR scheme is used as the nominal model in this analysis. However, the difference in the results obtained for the two schemes is also evaluated. Both DR and DS schemes are used for comparison with the differential particle-level result. In addition, we consider signal samples generated with MadGraph5_aMC@NLO v2.6.5 [31] to compare, at the particle level, the predictions that use the DR and DS schemes. Two other derivations from those approaches are also considered: the so-called “DR2” approach that includes the terms corresponding to the interference between tW and $\mathrm{t\bar{t}}$ processes, and an alternative way of implementing DS (later referenced as “DS dyn.”), where a dynamic factor is used to model the top quark resonance, instead of a fixed one [32]. The NLO QCD setup in POWHEG v2 is also used to simulate $\mathrm{t\bar{t}}$ events. The Drell–Yan (DY) background samples are simulated at NLO in QCD using MadGraph5_aMC@NLO v2.2.2, except in 2017, where it is simulated at LO in QCD using MadGraph5_aMC@NLO v2.4.2. The contributions from WW, WZ, and ZZ (referred to as VV) processes are simulated at NLO in QCD with POWHEG v2 or MadGraph5_aMC@NLO v2.2.2. Other contributions from W, Z, and γ boson production in association with $t\bar{t}$ events (referred to as $t\bar{t}V$) are simulated at NLO in QCD using MadGraph5_aMC@NLO v2.2.2. The small cross section processes of triboson production with different W, Z, and γ combinations are grouped together with the VV and $t\bar{t}V$ contributions and simulated at NLO in QCD with MadGraph5_aMC@NLO v2.2.2.

The lepton+jets events in the $t\bar{t}$ samples are used to estimate the contribution to the background from events with a jet incorrectly reconstructed as a lepton (electron or muon). Since the latter background contributions contain a lepton candidate that does not originate from a leptonic decay of a gauge boson, they are labelled non-W/Z.

The NNPDF 3.1 NNLO [33] PDF set is used in the simulation of all samples, except for the 2016 non-$t\bar{t}$ backgrounds for which 3.0 NNPDF NLO [34] is applied. The generators are interfaced in all cases with PYTHIA v8.230 [35], which is used to model the hadronisation and parton showering (PS). The underlying event is modelled with the CP5 tune [36] in all of the 2017–2018 samples. For 2016, the CP5 tune is used for the signal and $t\bar{t}$ background samples, whereas for the rest of the samples the CUETP8M1 tune [37] is taken. For comparison at the particle level, another signal sample where the POWHEG v2 generator is interfaced with HERWIG++ v2.7.1 (2016) and HERWIG 7 (2017–2018) [38–40] is used. This uses the EE5C tune [41] for 2016 and CH3 [42] for 2017–2018. For the samples generated with MadGraph5_aMC@NLO at LO (NLO) accuracy, double counting of partons from the matrix element calculations and PS described by PYTHIA v8.230 is removed using the MLM [43] (FxFx [44]) matching scheme. The nominal m_t is set to 172.5 GeV for all samples. For both the tW signal and $t\bar{t}$ background alternative samples were generated to estimate systematic uncertainties, which are obtained from the same generator (POWHEG v2) and PS simulation (PYTHIA v8.230). These uncertainties are described in detail in section 6.

The Geant4 package [45] is used to simulate the CMS detector response for all simulated samples. To compare with the measured data, the event yields in the simulated samples are normalised to the integrated luminosity using their theoretical cross sections. These are taken from calculations at NNLO for DY [46], approximate NNLO for tW events [12], and NLO for diboson events [47]. For the simulated $t\bar{t}$ sample, the full NNLO plus next-to-next-to-leading-logarithmic calculation [48], performed with the TOP++ 2.0 program [49], is used. The PDF uncertainty is added in quadrature to the uncertainty associated with the strong coupling constant (α_S) to obtain a $t\bar{t}$ production cross section of $832\,^{+20}_{-29}\,(\text{scale}) \pm 35\,(\text{PDF}+\alpha_S)$ pb, for $m_t = 172.5$ GeV.

The simulated samples include additional pp interactions in the same or nearby bunch crossings (pileup). A reweighting is applied in simulations to match the distribution of bunch crossings observed in the data. Assuming a total inelastic pp cross section of 69.2 mb [50], the average number of pileup interactions per bunch crossing are 23, 33, and 32 in 2016, 2017, and 2018, respectively.

3 Event selection

In the SM, top quarks decay nearly 100% of the time into a W boson and a bottom quark. The analysis described here uses events in the $e^{\pm}\mu^{\mp}$ final state, in which the W boson from the decay of the top quark and the W boson produced in association with the top quark both decay leptonically, one into an electron and a neutrino, and the other into a muon

JHEP07(2023)046

and a neutrino. This leads to a final state composed of two different-flavour leptons with opposite electric charge, one jet resulting from the fragmentation of a bottom quark, and two neutrinos.

Events are required to pass either a dilepton or single-lepton trigger with isolation requirements [26]. The dilepton triggers require events to contain either one electron with transverse momentum $p_T > 12\,\text{GeV}$ and one muon with $p_T > 23\,\text{GeV}$, or one muon with $p_T > 8\,\text{GeV}$ and one electron with $p_T > 23\,\text{GeV}$. The single-lepton triggers with one electron (muon) with $p_T > 27$ (24), 35 (24), and 32 (24) GeV for 2016, 2017, and 2018 are used to increase the efficiency. The combined trigger efficiency is measured using data events which pass the selection criteria given below, and which were collected with triggers based on the p_T imbalance in the event. It is found to be ≈98%. The trigger efficiency in simulated events is corrected to match that observed in data.

The particle-flow (PF) algorithm [51] aims to reconstruct and identify each individual particle in an event with an optimised combination of information from the various elements of the CMS detector. The primary vertex, which is the vertex corresponding to the hardest scattering in the event, is evaluated using tracking information alone, as described in section 9.4.1 of ref. [52]. Further requirements are imposed on the reconstructed and identified lepton and jet candidates obtained from the PF algorithm. Electrons [53] and muons [54] in the event are required to be well isolated and have $p_T > 20\,\text{GeV}$ and $|\eta| < 2.4$. Additional criteria are imposed on the impact parameter of the leptons in order to ensure that they come from the primary vertex. Electron candidates in the transition region between the barrel and endcap calorimeters, corresponding to $1.444 < |\eta| < 1.566$, are ignored because the electron reconstruction in this region is not optimal.

Events with W bosons decaying into τ leptons are considered as signal only if the τ leptons decay into electrons or muons that satisfy the selection requirements. In events with more than two leptons passing the selection, the two with the largest p_T are kept for further study. Jets are reconstructed from the PF candidates using the anti-k_T clustering algorithm [55, 56] with a distance parameter of 0.4. Jet energy corrections, derived from simulation, are applied so that the average response to jets matches the particle-level jets [57]. In situ measurements of the momentum balance in dijet, photon+jet, Z+jet, and multijet events are used to account for residual differences in the jet energy scale (JES) between data and simulation. In addition, jet energy resolution (JER) is corrected to reproduce that obtained from data [58].

Jets are required to have $p_T > 30\,\text{GeV}$ and $|\eta| < 2.4$. Jets with p_T between 20 and 30 GeV and $|\eta| < 2.4$ are referred to as "loose jets". The differences in these lower-p_T jets between the tW and $t\bar{t}$ distributions can be exploited for their separation. Jets are identified as coming from the fragmentation of bottom quarks (b jets) using the DeepJet algorithm [59, 60], with an operating point that yields identification efficiencies of ≈70% and misidentification probabilities of about 1% for light-quark and gluon jets. The missing transverse momentum vector $\vec{p}_T^{\text{miss}}$ is defined as the negative vector momenta sum of all reconstructed PF candidates, which include the jet energy corrections described above in an event, projected onto the plane perpendicular to the direction of the beam axis. Its magnitude is referred to as p_T^{miss}.

JHEP07(2023)046

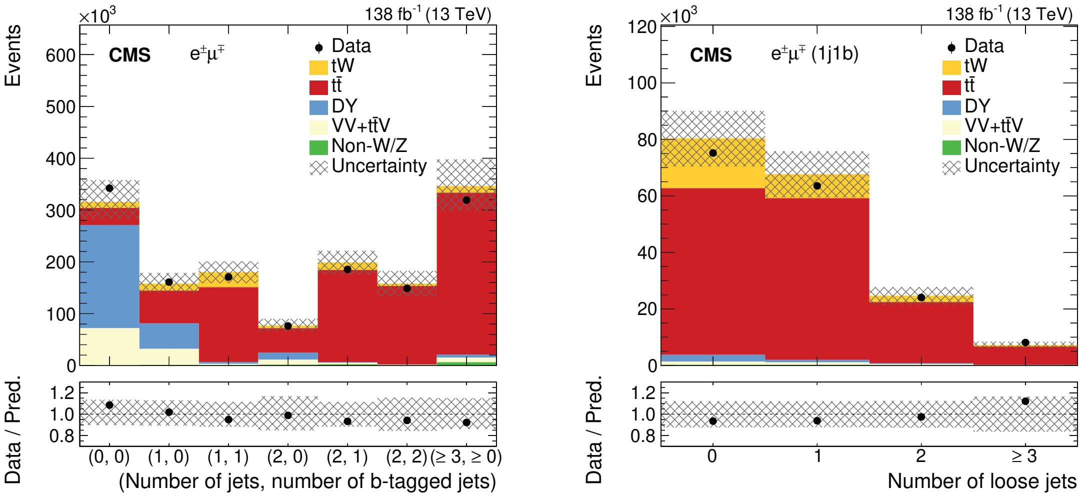

Figure 3. Left: the number of events from data (points) and predicted from simulation (coloured histograms) before the fit in the $e^{\pm}\mu^{\mp}$ sample as a function of the number of jets and b-tagged jets. Right: the number of loose jets per event in the $e^{\pm}\mu^{\mp}$ sample from the 1j1b region. The vertical bar on the points shows the statistical uncertainty in the data. The hatched band represents the sum of the statistical and systematic uncertainties before the fit. The lower panels show the ratio of data to the sum of the expected yields. The MC simulations are normalised to their theoretical cross section values as described in section 2.

Events are selected as belonging to the $e^{\pm}\mu^{\mp}$ final state if the two leptons with highest p_T passing the above selection criteria are an electron and a muon of opposite charge. The highest p_T (leading) lepton is required to have $p_T > 25\,\text{GeV}$. To reduce the contamination from DY production of τ lepton pairs with low dilepton invariant mass, the minimum invariant mass of all pairs of identified leptons (including leptons beyond the leading two) is required to be greater than 20 GeV. The remaining events are classified by the number of jets and identified b jets in the event, as shown in figure 3 (left). In the following, the notation njmb represents events with exactly n jets where m of them are identified as b jets. The most signal-enriched region is the 1j1b, but the contribution from tW is still only 20% that of $t\bar{t}$. For the inclusive measurement, we take advantage of the information from various regions (1j1b, 2j1b, and 2j2b), whereas for the differential measurement, only the 1j1b region is used. An additional selection criterion is applied to enhance the signal-to-background ratio in the differential measurement. Figure 3 (right) shows the distribution of the number of loose jets in the 1j1b events. The signal-to-background ratio is larger for events with zero loose jets. To minimise the relative contribution from the $t\bar{t}$ background, the events in the 1j1b region with zero loose jets are used for the differential measurement. Signal events contribute up to 22% of the total expected events in that region.

4 Methodology for the inclusive measurement

After the baseline event selection is performed, the presence of $t\bar{t}$ events is considerably larger than the tW signal in all event categories, as can be seen in figure 3 (left). The

JHEP07(2023)046

region with the best signal-to-background ratio is 1j1b, which consists mainly of tW and $t\bar{t}$ events. This region is used together with the 2j1b, which also contains a significant tW contribution, and 2j2b in a maximum likelihood (ML) fit to extract the tW signal. The 2j2b region is dominated by $t\bar{t}$ events and is used in the fit to constrain this background.

As there is no single observable that gives strong discrimination between $t\bar{t}$ and tW events, two independent boosted decision trees (BDTs [61, 62]), one for the 1j1b region and the other for the 2j1b region, are trained to discriminate between the tW signal and $t\bar{t}$ background. The BDTs outperform single-tree classifiers [63] by training a set of trees (forest) and taking their weighted vote as the prediction. Each tree is derived from the same training ensemble by reweighting their events to mitigate the statistical fluctuations and increase the overall stability. In this analysis, the BDT implementation is provided by the TMVA package [62], using gradient boost [62] as the boosting algorithm. The BDTs are trained and tested using a set of simulated samples that are statistically independent from the ones used in the signal extraction.

The input variables used in the BDTs are chosen depending on how well the MC simulation models the data and on their discrimination power. For the BDT in the 1j1b, the list of variables used in the training in order of importance are:

- $p_{\mathrm{T}}(\mathrm{e}^{\pm}, \mu^{\mp}, \mathrm{j})$: the magnitude of the transverse momentum of the dilepton + jet system.
- $C(\mathrm{e}^{\pm}, \mu^{\mp}, \mathrm{j})$: centrality, which is defined as $\sin\theta$, where θ is the polar angle of the total momentum of the system.
- $m(\mathrm{e}^{\pm}, \mu^{\mp}, \mathrm{j}, \vec{p}_{\mathrm{T}}^{\,\mathrm{miss}})$: invariant mass of the dilepton + jet + $\vec{p}_{\mathrm{T}}^{\,\mathrm{miss}}$ system.
- Leading loose jet p_{T}: if there are no loose jets, this variable is set to 0.
- Jet p_{T}.
- Presence of loose jets in the event: the result is either yes or no.

The order of importance is determined by counting how often each variable is used to split the decision tree nodes. The counts are weighted by the square of the separation gain achieved by the variable and by the number of events in the node. Figure 4 shows the data-MC agreement of the four most discriminating variables in the BDT for 1j1b, where good agreement is observed. The same applies for the remaining distributions of the presence of loose jets and the jet p_{T}, and for the input variables of the BDT trained in the 2j1b region.

The input variables listed in order of importance in the BDT for 2j1b are:

- $\Delta R(\ell_1, \mathrm{j}_1)$: separation in η-φ space between the leading lepton and leading jet, where φ is the azimuthal angle.
- $\Delta R(\ell_{12}, \mathrm{j}_{12})$: separation in η-φ space between the dilepton and dijet systems.
- Second-highest jet p_{T} (subleading).

JHEP07(2023)046

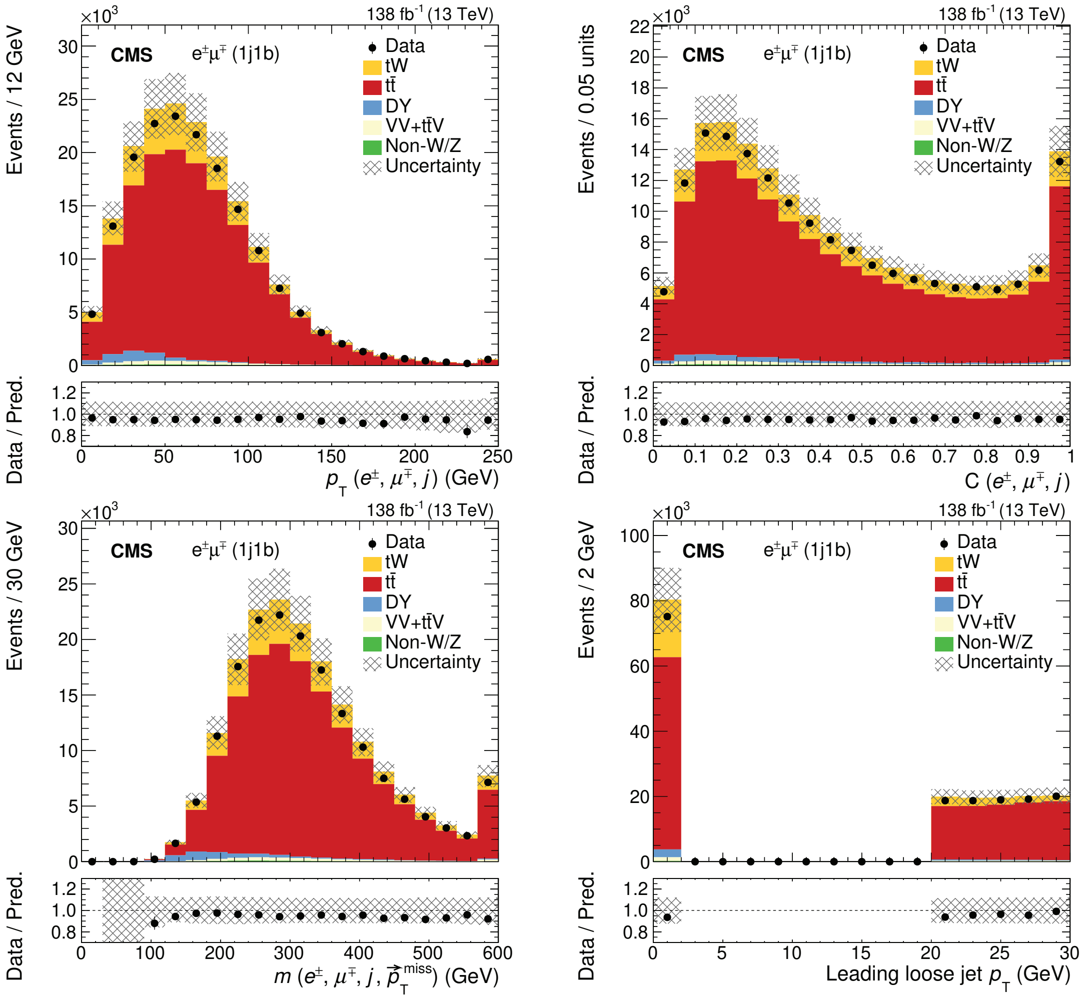

Figure 4. Distributions from data (points) and MC simulations (coloured histograms) of the four most discriminating variables used for the BDT training of the 1j1b region: (upper left) the magnitude of the transverse momentum of the dilepton + jet system; (upper right) the centrality, defined in the text, of the dilepton + jet system; (lower left) the invariant mass of the dilepton + jet + $\vec{p}_T^{miss}$ system; and (lower right) the p_T of the leading loose jet. The last bin of each distribution includes the overflow events. The first bin in the lower right plot contains events with 0 loose jets. The vertical bars on the points give the statistical uncertainty in the data, and the grey bands represent the sum of the statistical and systematic uncertainties in the MC predictions. The lower panels show the ratio of the data to the sum of the MC predictions. The MC simulations are normalised to their theoretical cross section values as described in section 2.

Three distributions are considered in the ML fit: the BDT output distributions in the 1j1b and 2j1b regions, and the p_T distribution of the subleading jet in the 2j2b region. This last variable is sensitive to JES variations and is useful in constraining this systematic uncertainty. The binning of the BDT output distribution is chosen such that each bin contains about the same number of $t\bar{t}$ events. This avoids the presence of low-statistic bins in the background estimation, helping to constrain the systematic uncertainties. The fit is performed simultaneously with the three regions. The uncertainties are included using nuisance parameters, one for each source of systematic uncertainty, correlated across all regions, which parameterise the effect of the given source on the expected signal and background yields.

The likelihood used in this ML fit, $\mathcal{L}(\vec{n}|\mu, \vec{\theta})$, is a function of the signal strength μ, defined as the ratio of the measured and expected SM cross sections $\mu = \sigma_{\mathrm{tW}}/\sigma_{\mathrm{tW}}^{\mathrm{SM}}$, the observed number of events in each bin $\vec{n}$, and a set of nuisance parameters $\vec{\theta}$ that parameterise the systematic uncertainties. It is constructed as the product of Poisson probabilities corresponding to the number of events in each bin of the distributions. Additionally, the systematic uncertainties are introduced in the likelihood multiplied by the prior $p_j(\theta_j)$ of each nuisance parameter θ_j. In this analysis, a log-normal probability density function is used for nuisance parameters affecting the normalisation of different signal and background processes, and a Gaussian distribution is employed for the shape uncertainties. The best fit value for μ is obtained by maximising the likelihood function with respect to all its parameters. The ML fits are implemented with software based on RooStats [64]. The MC statistical uncertainties are incorporated using the Barlow–Beeston method [65, 66]. Other uncertainties that might affect both the normalisation and shape of the distributions are introduced using specific nuisance parameters [66, 67] with a Gaussian function prior.

5 Methodology for the differential measurement

The spectra of observables are distorted by the response and acceptance of the detector. Unfolding techniques must, therefore, be used to determine the actual distributions without the detector effects so that these can be directly compared with theoretical predictions. The data affected by these distortions are said to be at detector level. The parton level is defined by the particles produced after the generation of the hard-scattering process. If the information from the PS and hadronisation simulations is added, this then gives the particle level.

The measured distributions are unfolded from the detector level to the particle level. Unfolding to particle level instead of parton level reduces the migration and efficiency corrections, and allows the fiducial region to be defined in close correspondence with the event selection of the analysis.

The identification of particle-level objects is summarised in table 1. These objects are constructed using stable (i.e. with a lifetime larger than 30 ps) generated particles following the conventions given in ref. [68]. Muons and electrons not coming from hadronic decays (prompt leptons) are "dressed" by taking into account the momenta of nearby photons within a $\Delta R < 0.1$ cone, where ΔR is the separation in η-φ space between the muon or electron and the photon. Jets are clustered from all of the stable particles excluding prompt electrons, prompt muons, prompt photons, and neutrinos, using the anti-k_{T} algorithm with a distance parameter of $R = 0.4$. The information of the intermediate hadrons and τ leptons is preserved inside the jets and used to determine whether a jet originates from the fragmentation of a heavy-flavour quark (bottom or charm) or whether it is a decay product of a τ lepton. With these requirements, a fiducial region is defined as described in table 2. Requiring exactly one b jet reduces the potential to have events from the doubly-resonant

Object	p_{T} (GeV)	$\|\eta\|$
Muons	>20	<2.4
Electrons	>20	<2.4, excluding [1.444–1.566]
Jets	>30	<2.4
Loose jets	>20, <30	<2.4

Table 1. Selection requirements for particle-level objects.

Number of leptons	≥2
Leading lepton p_{T}	>25 GeV
Invariant mass of all dilepton pairs	>20 GeV
Number of jets	1
Number of loose jets	0
Number of b jets	1

Table 2. Definition of the fiducial region.

diagrams. Those events, more affected by the interference between processes, are expected to have a larger jet multiplicity. The differences between the various models used to treat the interference are expected to be higher when the presence of events from doubly-resonant diagrams is larger, and vice versa. For the unfolded distributions in the fiducial region, as shown in figure 8, all MC simulations show very similar distributions. Therefore, this choice of fiducial region reduces these effects and the accompanying modelling uncertainty associated with the interference treatment (see section 6).

The signal extraction and the unfolding for the fiducial differential cross section measurement are performed with an ML fit designed as follows. The parameters of interest are the strengths of the signal process in each bin of the particle-level distribution. The signal sample is divided into as many contributions as there are particle-level bins. There is a 7% contribution to the signal region from nonfiducial events. We treat these events as a background so the strength associated with them is not a parameter of interest. One nuisance parameter for each systematic uncertainty source is added to the fit.

The differential cross section is measured as a function of the following physical observables:

- leading lepton p_{T};
- jet p_{T};
- $\Delta\varphi(\mathrm{e}^{\pm}, \mu^{\mp})$: the azimuthal angle difference between the two leptons;
- $p_z(\mathrm{e}^{\pm}, \mu^{\mp}, \mathrm{j})$: the longitudinal momentum component of the dilepton + jet system;
- $m(\mathrm{e}^{\pm}, \mu^{\mp}, \mathrm{j})$: the invariant mass of the dilepton + jet system; and,
- $m_{\mathrm{T}}(\mathrm{e}^{\pm}, \mu^{\mp}, \mathrm{j}, \vec{p}_{\mathrm{T}}^{\text{miss}})$: the transverse mass of the dilepton + jet + $\vec{p}_{\mathrm{T}}^{\text{miss}}$ system. For a collection of particles with transverse momentum $\vec{p}_{\mathrm{T},i}$, m_{T} is defined as:

$$m_{\mathrm{T}} = \sqrt{\left(\sum_i |\vec{p}_{\mathrm{T},i}|\right)^2 - \left|\sum_i \vec{p}_{\mathrm{T},i}\right|^2}. \qquad (5.1)$$

The first two variables shown above provide information on the kinematic properties of the events. The $\Delta\varphi(e^{\pm}, \mu^{\mp})$ variable probes the kinematic and polarisation correlations between the top quark and W boson. The p_z distribution can be used to study the boost of the tW system. The last two variables, the dilepton + jet invariant mass and m_T, are sensitive to the invariant mass of the tW system. The distributions from the data and simulation for these six variables in the signal region are shown in figure 5. As in the case of figures 3 and 4, overall there is good agreement within the uncertainties between the data and simulation, though the data are consistently lower than the predicted values.

The measurement is performed using all three years of data taking. The detector response is estimated using the response matrices, which are similar for the three years, with the matrices being almost diagonal. Thus, the measurement is performed directly using the combined data set and without need of regularisation. After the ML fit, the result is normalised to the fiducial cross section (obtained from the summation of the contents of the bins), and the bin width. The uncertainties are propagated taking into account the correlations across bins after the fit. The Asimov data set has been used to verify the closure and performance of the unfolding procedure.

6 Systematic uncertainties

In addition to statistical uncertainties, the measurements of the inclusive and differential tW cross sections are affected by systematic uncertainties that originate from both detector effects and theoretical assumptions. Each source of systematic uncertainty is assessed individually by suitable variations of the simulations or by variations of parameter values in the analysis within their estimated uncertainties. The systematic uncertainties are introduced in the ML fits as nuisance parameters. All experimental sources are applied to all processes.

The following text describes the sources considered for both the inclusive and differential analyses. Since we are considering data and simulation samples from different years, we indicate whether each uncertainty is correlated or not from year to year. In the case of the modelling uncertainties, we also indicate if they are correlated among the processes or not. Both normalisation and shape effects of all sources are considered apart from the background normalisation and integrated luminosity, which have only rate uncertainties. Effects of all sources in the estimation of the number of events that are not in the fiducial region are taken into account in the maximum likelihood fit, as well as their correlation with other uncertainties.

6.1 Experimental uncertainties

JES and JER: the uncertainty due to the limited knowledge of the JES and JER is determined by varying the scale and resolution within the uncertainties in bins of the jet p_T and η, typically by a few percent [57]. The JES and JER uncertainties are propagated to $\vec{p}_T^{miss}$. The JES uncertainty sources are separated into various components that are correlated or uncorrelated across years in different groups. The JER uncertainty is uncorrelated across years.

JHEP07(2023)046

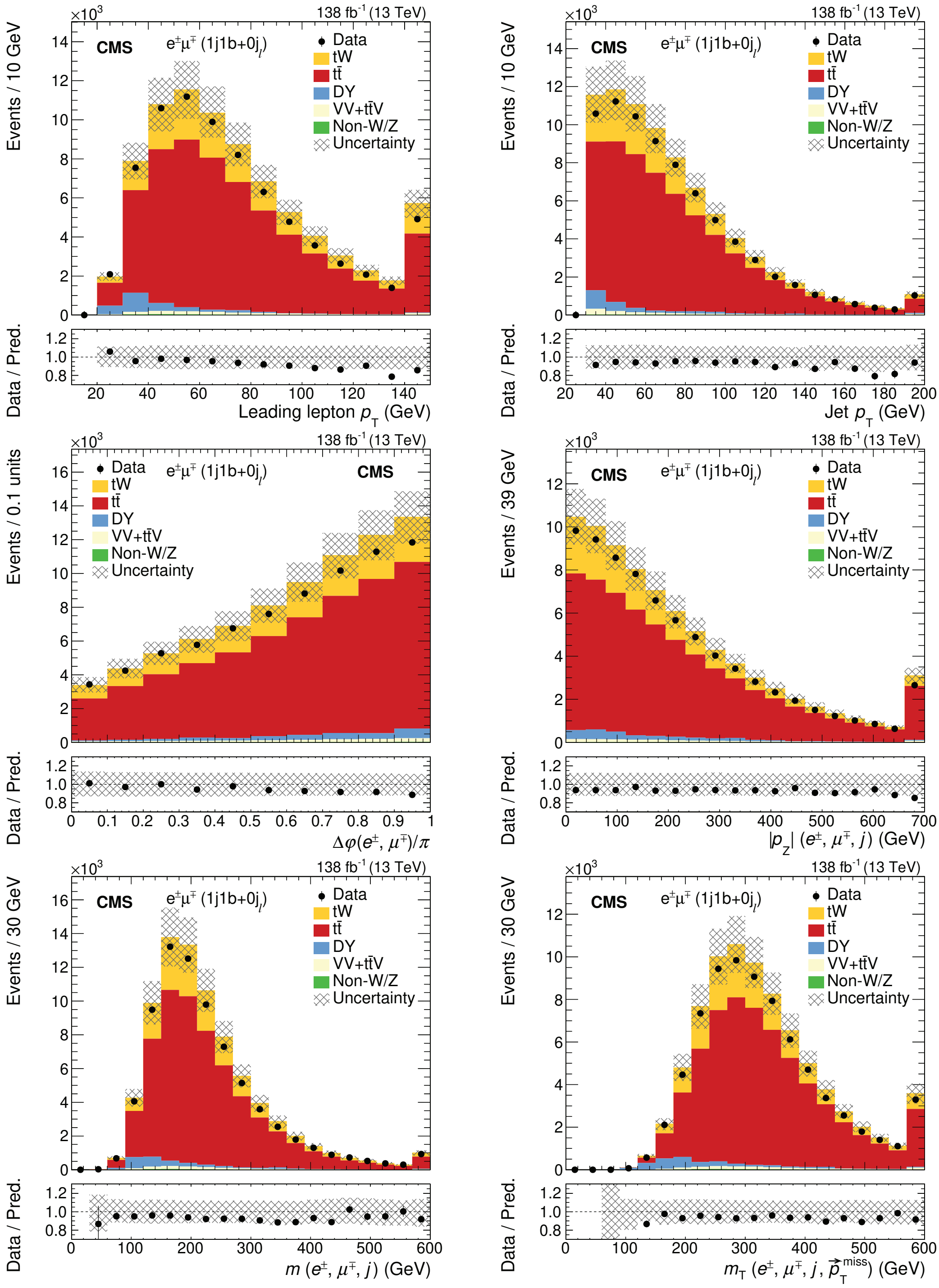

Figure 5. The measured distributions from data (points) and MC simulations (coloured histograms) of the six observables used to measure the tW differential cross sections. Signal events in the 1j1b region with 0 loose jets ($0j_l$) are selected. The last bin of each distribution contains the overflow events. The vertical bars on the data show the statistical uncertainty. The hatched band displays the sum of the statistical and systematic uncertainties in the MC predictions before the fit. The lower panels show the ratio of the data to the sum of the MC expectations. The MC simulations are normalised to their theoretical cross section values as described in section 2.

JHEP07(2023)046

Unclustered energy: the effect of unclustered energy from the calorimeters on $\vec{p}_{\mathrm{T}}^{\mathrm{miss}}$ is taken into account through the momentum resolution of the various PF candidates [51, 69, 70]. This is correlated across years.

b tagging: the uncertainties resulting from the b tagging data-to-simulation scale factors (SFs) are assessed by varying them, within their uncertainties, for the b, c, light-flavoured, and gluon jets. These uncertainties vary with the p_{T} and η of the jet and amount to approximately 2% for b-tagged jets and 10% for misidentified jets [71], as determined in simulated $\mathrm{t\bar{t}}$ events. They are split into one correlated source (the systematic effect) across years, and one uncorrelated source (the statistical effect) per year for heavy-flavour (b and c) tagging and light-flavoured/gluon jet misidentification cases.

Trigger and lepton identification: the uncertainties in the trigger and lepton identification and isolation are estimated by varying the data-to-simulation SFs by their uncertainties. These are about 0.7% (trigger) and 1.5% (lepton identification and isolation), with some dependence on the lepton p_{T} and η. The trigger uncertainties contain statistical sources (from both the MC simulations and data used) and systematical ones (estimating the effect of the event topology used to derive them and the consequences of selecting triggers based on the p_{T} imbalance of the events). The lepton identification and isolation scale factors are derived through the tag-and-probe method [72] as a function of the lepton p_{T} and η. For muons, an additional uncertainty of 0.5% is added in quadrature to account for the extrapolation from the phase space in which the isolation SFs are measured and the phase space for the analysis. The trigger and the statistical component of the muon identification uncertainties are uncorrelated across years, while the rest of the uncertainties are correlated. The identification and isolation uncertainties of muons are considered separately. In the case of electron identification and reconstruction uncertainties, they are taken as correlated across years.

Muon momentum scale: to account for the uncertainties in the muon momentum scale, the momentum of the muons is varied by its uncertainties [54]. These are uncorrelated across years. The experimental uncertainties in the electron energy (both scale and resolution) have been found to have a negligible effect and are thus not considered.

Pileup: the uncertainty assigned to the number of pileup interactions in simulation is obtained by varying the inelastic pp cross section within its uncertainty of 4.6% [73]. This uncertainty is correlated across the three years.

Luminosity: the uncertainty in the integrated luminosity is estimated to be 1.2, 2.3, and 2.5% for 2016 [74], 2017 [75], and 2018 [76], respectively, with a combined uncertainty of 1.6%. The uncertainty is partially correlated across the years.

L1 prefiring: in 2016–2017, the L1 trigger from the electromagnetic calorimeter from the forward endcap region ($|\eta| > 2.4$) of the CMS detector showed a gradual shift in the timing of its inputs. This caused a effect known as “prefiring”, where particles were assigned to previous collisions. This inefficiency only affects events having jets with high pseudorapidity ($2.4 < |\eta| < 3.0$) and high p_T (>100 GeV). Events from these years are corrected through a reweighting determined from an unbiased data sample. An uncertainty equal to 20% of the correction is taken. This uncertainty source is uncorrelated across the two years.

6.2 Modelling uncertainties

The impact of theoretical assumptions in the modelling is determined by repeating the analysis and replacing the standard POWHEG + PYTHIA8 $t\bar{t}$ or tW simulation by dedicated simulation samples with altered parameters, or by reweighting the nominal samples.

Matrix element (ME) scales: the uncertainty in the modelling of the hard process is only considered for $t\bar{t}$ and tW events and is assessed by changing independently the μ_R and μ_F scales in the POWHEG sample by factors of 2 and 0.5 relative to their common nominal value. Unphysical variations of μ_R and μ_F, where the nominal values are shifted in opposite directions, are not considered. This uncertainty is correlated across years, and is performed separately for $t\bar{t}$ and tW events.

Parton shower (PS): to take into account the PS uncertainties, different effects are studied:

- Underlying event: PYTHIA parameters are tuned to the measurements of the underlying event [36, 77]. These account for nonperturbative QCD effects. They are varied up and down in simulated $t\bar{t}$ and tW events. This variation is correlated across years and between $t\bar{t}$ and tW events.
- ME/PS matching: the uncertainty in the combination of the ME calculation with the PS in simulated $t\bar{t}$ events is estimated from the variation, within its uncertainties, of the POWHEG parameter $h_{\mathrm{damp}} = \left(1.379\,^{+0.926}_{-0.505}\right) m_t$ [36, 78]. This parameter regulates the damping of real emissions in the NLO calculation when matching to the PS [77]. This variation is correlated across years and is only considered for $t\bar{t}$ events.
- Initial- and final-state radiation scales: the PS scale used for the simulation of the initial- and final-state radiations is varied up and down by a factor of two and only considered for $t\bar{t}$ and tW events. These variations are motivated by the uncertainties in the PS tuning [77]. This variation is correlated across years for the final-state radiation in the $t\bar{t}$ and tW events, and is treated separately for initial-state radiation.
- Colour reconnection: the parameterisation of colour reconnection has been studied in ref. [79]. A simulation including colour reconnection of early resonant decays (ERD) is used as the reference model. The uncertainties that arise from ambiguities in modelling are estimated by comparing with two alternative models of colour reconnection: a model with string formation beyond leading colour,

and a model in which the gluons can be moved to another string [80]. All models are tuned to measurements of the underlying event [77, 78]. The different models are included in the ML fits. This variation is correlated across years and between $\mathrm{t\bar{t}}$ and tW events.

PDFs and α_S: the uncertainty from the choice of PDF set is determined by reweighting the samples of simulated $\mathrm{t\bar{t}}$ and tW events using 100 NNPDF3.1 replicas [33]. Since they represent the contents of a diagonalised Hessian matrix, the variations are summed quadratically. We then quadratically add the uncertainty in the α_S parameter [33]. This uncertainty is correlated across years and between $\mathrm{t\bar{t}}$ and tW events.

Top quark mass: the nominal m_t of 172.5 GeV is modified by ± 1 GeV and this is propagated to the MC simulations. This corresponds to twice the uncertainty in m_t from CMS [81]. The difference with respect to the nominal results is taken as the uncertainty and is only considered for $\mathrm{t\bar{t}}$ and tW events. This variation is correlated across years and between $\mathrm{t\bar{t}}$ and tW events.

Top quark p_T: previous measurements of the differential cross section for $\mathrm{t\bar{t}}$ production have shown that the top quark has a lower average p_T value than predicted by the POWHEG simulation [82–84]. Scale factors are obtained by comparing the generated distributions of the top quark p_T with data unfolded to parton level. The difference between corrected and uncorrected shapes is taken as the uncertainty associated with the mismodelling of the top quark p_T, leaving the nominal $\mathrm{t\bar{t}}$ events untouched. This variation is correlated across years and only affects $\mathrm{t\bar{t}}$ events.

DR / DS different methods: the difference between the DR and DS methods used to estimate the uncertainties in the tW simulation. This variation is correlated across years.

6.3 Background normalisation uncertainties

An uncertainty of 4% [85] is taken as the uncertainty in the normalisation of the inclusive $\mathrm{t\bar{t}}$ cross section. For the $\mathrm{t\bar{t}}$V, VV, and the non-W/Z backgrounds, a normalisation uncertainty of 50% is used, as in ref. [18]. Using the differences between the data and simulations in regions of phase space close to the signal region, a 10% uncertainty is used for the DY background.

7 Results

7.1 Inclusive measurement

The measured value for $\mu = \sigma_{\mathrm{tW}}/\sigma_{\mathrm{tW}}^{\mathrm{SM}}$ is obtained by maximising the likelihood function with respect to all its parameters. The fit is performed using the BDT discriminants in the 1j1b and 2j1b regions and the subleading jet p_T distribution in the 2j2b region.

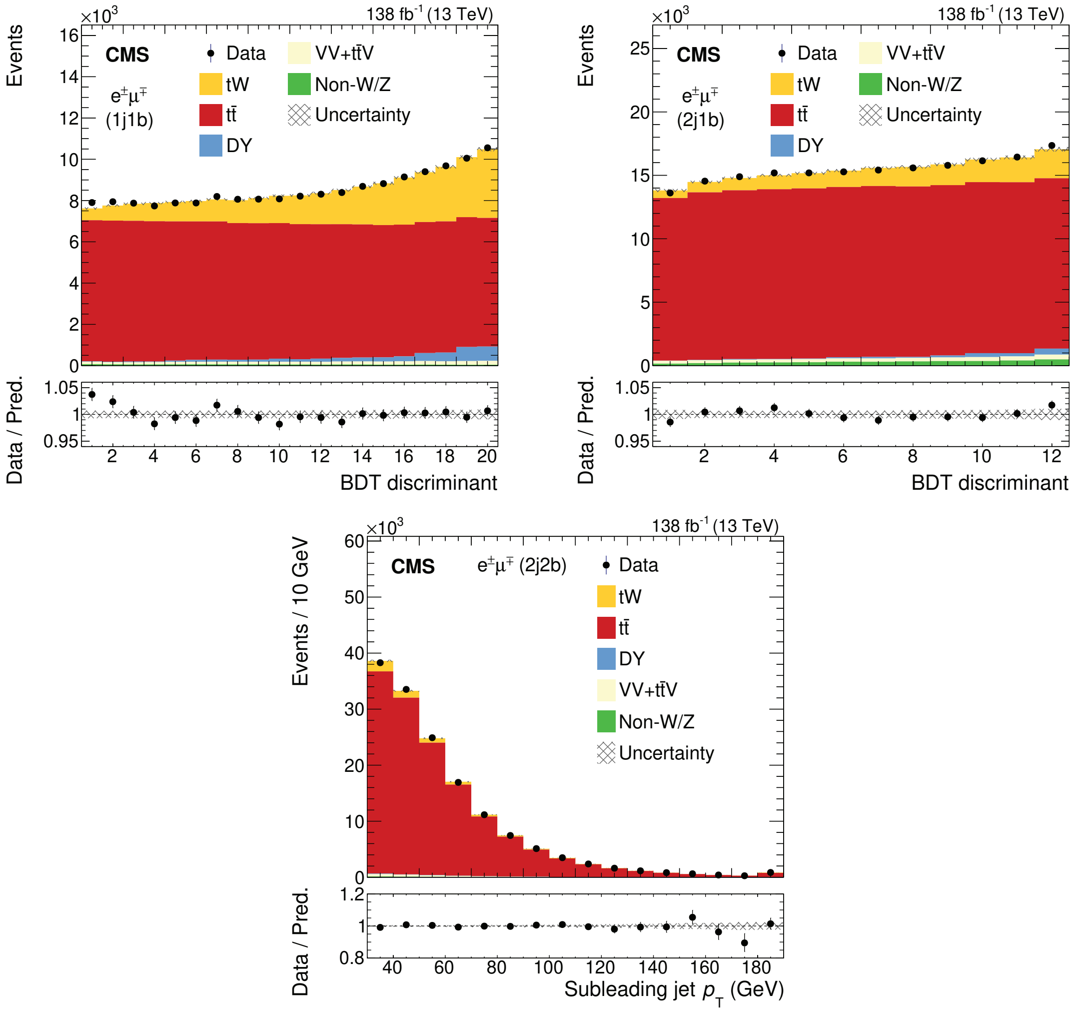

Figure 6. The distributions of the BDT outputs for events in the 1j1b (upper left) and 2j1b (upper right) regions, and the subleading jet p_T for the 2j2b region (lower). The data (points) and the MC predictions (coloured histograms) after the fit are shown. The vertical bars on the points represent the statistical uncertainty in the data, and the hatched band the total uncertainty in the MC prediction. The lower panels display the ratio of the data to the sum of the MC (points) predictions after the fit, with the bands giving the corresponding uncertainties.

The resulting signal strength is consistent with the SM expectations, corresponding to an inclusive cross section of

$$\sigma_{\mathrm{tW}} = 79.2 \pm 0.9\,(\mathrm{stat})\,^{+7.7}_{-8.0}\,(\mathrm{syst}) \pm 1.2\,(\mathrm{lumi})\,\mathrm{pb}. \tag{7.1}$$

The distributions of the BDT discriminants in the 1j1b and 2j1b regions and the subleading-jet p_T distribution in the 2j2b region after the fit are shown in figure 6. The observed and MC predicted event yields in the three regions are given in table 3.

The 20 largest impacts on the signal strength and the corresponding nuisance parameters are shown in figure 7. The impact is defined as the shift $\Delta\hat{\mu}$ induced in μ when the nuisance parameter θ is varied by ± 1 standard deviation (σ) around its best fit value.

Process	1j1b	2j1b	2j2b
tW	$31\,600 \pm 600$	$16\,600 \pm 500$	$5\,500 \pm 200$
$\mathrm{t\bar{t}}$	$131\,200 \pm 500$	$160\,300 \pm 600$	$141\,100 \pm 400$
Drell–Yan	$3\,990 \pm 190$	$1\,630 \pm 100$	260 ± 20
VV+$\mathrm{t\bar{t}}$V	$2\,800 \pm 300$	$3\,300 \pm 500$	$1\,700 \pm 400$
Non-W/Z	$1\,140 \pm 150$	$3\,700 \pm 700$	470 ± 120
Total	$170\,800 \pm 300$	$185\,400 \pm 400$	$149\,100 \pm 300$
Data	$170\,900 \pm 400$	$185\,400 \pm 400$	$148\,900 \pm 400$

Table 3. The number of observed and MC predicted events after the fit in the 1j1b, 2j1b, and 2j2b regions. The statistical uncertainties in the data and the total uncertainties in the predictions are given.

Variable	PH DR + P8	PH DS + P8	PH DR + H7
Leading lepton p_{T}	0.02	0.01	0.03
Jet p_{T}	0.14	0.27	0.01
$\Delta\varphi(\mathrm{e}^{\pm},\mu^{\mp})/\pi$	0.26	0.29	0.32
$p_z(\mathrm{e}^{\pm},\mu^{\mp},\mathrm{j})$	0.70	0.77	0.82
$m_{\mathrm{T}}(\mathrm{e}^{\pm},\mu^{\mp},\mathrm{j},\vec{p}_{\mathrm{T}}^{\,\mathrm{miss}})$	0.54	0.60	0.59
$m(\mathrm{e}^{\pm},\mu^{\mp},\mathrm{j})$	0.03	0.02	0.28

Table 4. The p-values from the goodness-of-fit tests comparing the six differential cross section measurements with the predictions from POWHEG (PH) + PYTHIA 8 (P8) DR and DS and POWHEG + HERWIG7 (H7) DR. The complete covariance matrix from the results and the statistical uncertainties in the predictions are taken into account.

The leading uncertainties are the JES corrections, the normalisation of the non-W/Z background, the ME scales of the tW process, and the modelling of the final-state radiation for $\mathrm{t\bar{t}}$ and tW. Figure 7 also shows the pulls of the nuisance parameters, $(\hat{\theta} - \theta_0)/\Delta\theta$, where $\hat{\theta}$ and θ_0 are the values after and before the fit of the nuisance parameter θ, and $\Delta\theta$ its uncertainty before the fit. Several nuisance parameters, such as the b tagging efficiency and jet energy corrections, are significantly constrained in the fit due to their effect on the jet multiplicity. The ME scales of the $\mathrm{t\bar{t}}$ process are also constrained because of the large presence of $\mathrm{t\bar{t}}$ events in all the regions used in the fit. These constraints help in the reduction of the uncertainties during the fit, yielding the most precise measurement of the inclusive tW cross section yet published.

7.2 Normalised fiducial differential cross section measurements

The tW differential cross sections, normalised to the total fiducial cross section $\sigma_{\mathrm{fid.}}$ (obtaining by summing the contents of the particle level bins), are shown in figure 8 from the data and the MC predictions. Tables 4 and 5 give the p-values from the χ^2 goodness-of-fit tests done for the six distributions, using the different MC generators and taking into account the full covariance matrix of each result, as well as the statistical uncertainties of the MC predictions. The full covariance matrix is obtained by normalising the covariance

JHEP07(2023)046

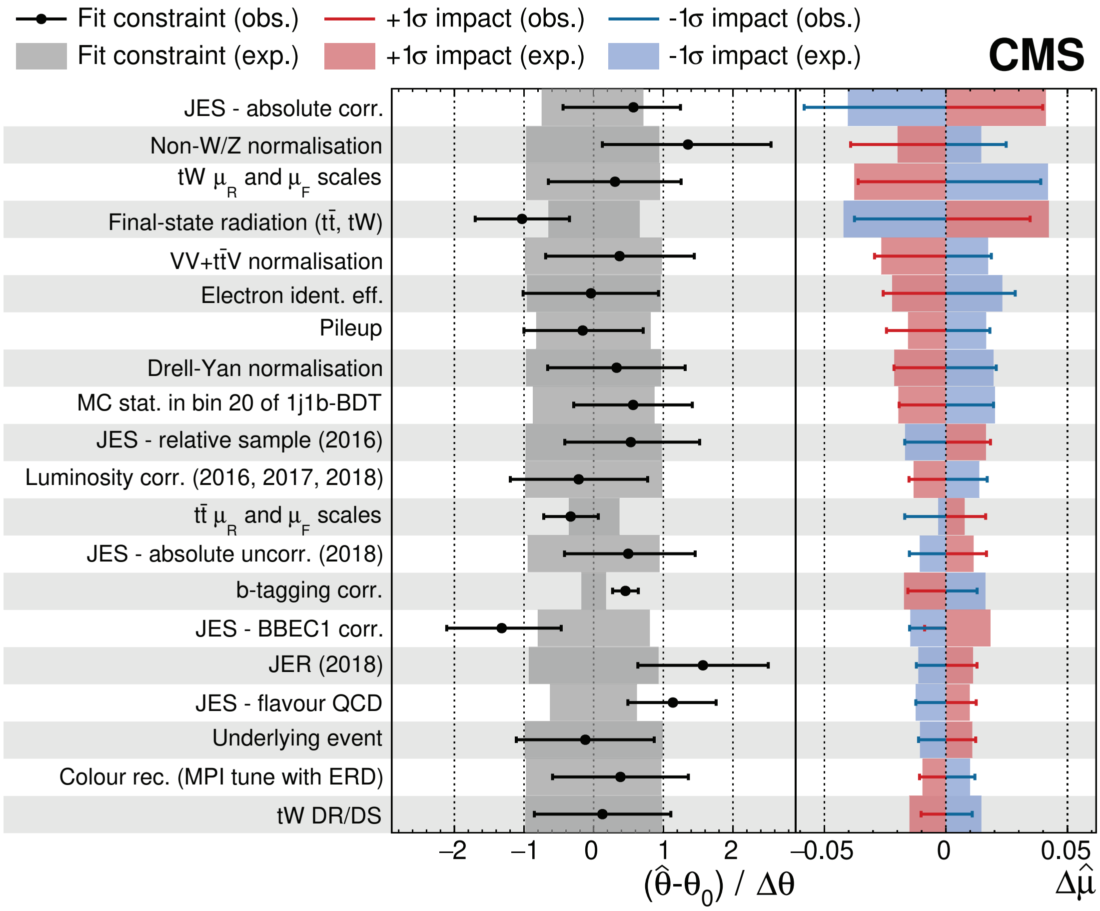

Figure 7. The 20 largest impacts $\Delta\hat{\mu}$ (right column) and pulls $(\hat{\theta} - \theta_0)/\Delta\theta$ (middle column) of the nuisance parameters listed in the left column from the ML fit used to determine the inclusive tW cross section. The horizontal bars on the pulls show the ratio of the uncertainties of the fit result to the previous ones, effectively giving the constraint on the nuisance parameter. The label "corr." refers to the correlated component of the uncertainty over the three years and "uncorr." the uncorrelated component for each year. The JES uncertainties are divided into several sources, where "JES-Absolute" groups contributions from scale corrections in the barrel, pileup corrections, and initial- and final-state radiation corrections; "JES-Relative sample" encodes the uncertainty in the η-dependent calibration of the jets; "JES-BBEC1" refers to pileup removal in the barrel (BB) and the first part of the endcaps ($1.3 < |\eta| < 2.5$; EC1) and also a contribution from scale corrections in the barrel; and "JES-Flavour QCD" comes from the corrections applied to correct the different detector response to gluon and quark jets.

matrix extracted from the maximum likelihood fit to the measured fiducial cross section. These tests show a poorer compatibility in the leading lepton p_T, $m(e^{\pm}, \mu^{\mp}, j)$, and jet p_T distributions with the nominal POWHEG + PYTHIA8 DR prediction than in the other variables. In most of the cases, the p-values determined from the distributions of all the variables are similar for the other expectations. When comparing data to the predictions, there is a slight disagreement in the leading lepton p_T and the $\Delta\varphi(e^{\pm}, \mu^{\mp})$ differential cross sections. Other CMS measurements have measured similar tensions in the top quark p_T [86]

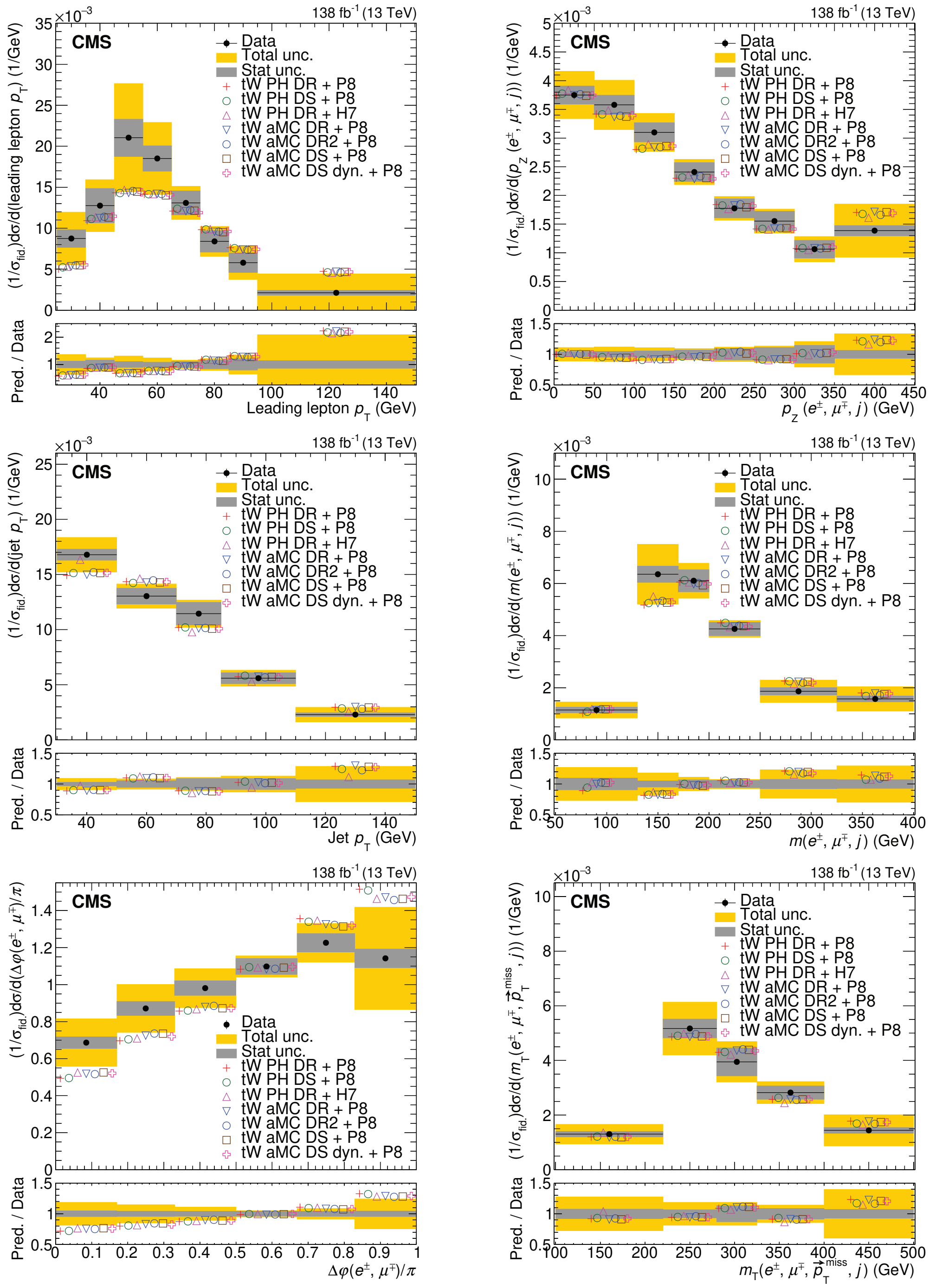

Figure 8. Normalised fiducial differential tW production cross section as functions of the p_T of the leading lepton (upper left), $p_z(e^\pm, \mu^\mp, j)$ (upper right), p_T of the jet (middle left), $m(e^\pm, \mu^\mp, j)$ (middle right), $\Delta\varphi(e^\pm, \mu^\mp)$ (lower left), and $m_T(e^\pm, \mu^\mp, j, \vec{p}_T^{\rm miss})$ (lower right). The vertical bars on the points give the statistical uncertainty in the data, the horizontal bars show the bin width. Predictions from POWHEG (PH) + PYTHIA 8 (P8) DR and DS, POWHEG + HERWIG7 (H7) DR, MADGRAPH5_aMC@NLO (aMC) + PYTHIA 8 DR, DR2, DS, and DS with a dynamic factor are also shown. The grey band represents the statistical uncertainty and the orange band the total uncertainty. In the lower panels, the ratio of the predictions to the data is shown.

JHEP07(2023)046

Variable	aMC DR + P8	aMC DR2 + P8	aMC DS + P8	aMC DS dyn. + P8
Leading lepton p_{T}	0.05	0.04	0.03	0.07
Jet p_{T}	0.15	0.11	0.14	0.12
$\Delta\varphi(\mathrm{e}^{\pm}, \mu^{\mp})/\pi$	0.33	0.40	0.37	0.32
$p_z(\mathrm{e}^{\pm}, \mu^{\mp}, \mathrm{j})$	0.76	0.86	0.84	0.82
$m_{\mathrm{T}}(\mathrm{e}^{\pm}, \mu^{\mp}, \mathrm{j}, \vec{p}_{\mathrm{T}}^{\text{miss}})$	0.49	0.51	0.48	0.52
$m(\mathrm{e}^{\pm}, \mu^{\mp}, \mathrm{j})$	0.09	0.12	0.10	0.14

Table 5. The p-values from the goodness-of-fit tests comparing the six differential cross section measurements with the predictions from MadGraph5_aMC@NLO (aMC) + PYTHIA 8 DR, DR2, DS, and DS with a dynamic factor. The complete covariance matrix from the results and the statistical uncertainties in the predictions are taken into account.

and $\Delta\varphi(\mathrm{e}^{\pm}, \mu^{\mp})$ [87] variables. All methods, DR, DR2, DS, and DS with a dynamic factor, show similar compatibility with the measurements, as well as small differences among them. This is also true for the DR predictions interfaced with HERWIG 7. The uncertainties, roughly 10–50% in most cases, depending on the distributions and bins, are dominated by the systematic uncertainties, as in the case of the inclusive measurement.

8 Summary

Inclusive and normalised differential cross sections for the production of a top quark in association with a W boson are measured in proton-proton collision data at $\sqrt{s} = 13\,\text{TeV}$. The data, corresponding to an integrated luminosity of $138\,\text{fb}^{-1}$, were recorded by the CMS detector, contain events with an electron and a muon of opposite charge.

For the inclusive measurement, the events have been categorised depending on the number of jets and jets originating from the fragmentation of bottom quarks. The signal is measured using a maximum likelihood fit to the distribution of boosted decision tree discriminants in two of the categories, and to the transverse momentum (p_{T}) distribution of the second-highest-p_{T} jet in a third category. The measured inclusive cross section is $79.2 \pm 0.9\,(\text{stat})\,^{+7.7}_{-8.0}\,(\text{syst}) \pm 1.2\,(\text{lumi})\,\text{pb}$, with a total relative uncertainty of about 10%. This is the most precise measurement of this quantity yet published. The leading uncertainty sources are the jet energy scale corrections, the normalisation in the non-W/Z background, the matrix element scales of the tW process, and the modelling of the final-state radiation in the $\mathrm{t\bar{t}}$ and tW processes.

The differential cross section measurements are performed as a function of six kinematical observable of the events in the fiducial phase space corresponding to the selection criteria. The results have relative uncertainties in the range of 10–50%, depending on the measured observable, with larger values in the tails of the distributions. The uncertainties are overall systematically dominated, with the modelling sources being the dominant ones. There is overall good agreement between the measurements and the predictions from the different event generators. The different approaches used to simulate the tW events give similar values in all the distributions, which points to small effects of $\mathrm{tW/t\bar{t}}$ interference on these distributions in the defined fiducial region.

JHEP07(2023)046

Acknowledgments

We congratulate our colleagues in the CERN accelerator departments for the excellent performance of the LHC and thank the technical and administrative staffs at CERN and at other CMS institutes for their contributions to the success of the CMS effort. In addition, we gratefully acknowledge the computing centres and personnel of the Worldwide LHC Computing Grid and other centres for delivering so effectively the computing infrastructure essential to our analyses. Finally, we acknowledge the enduring support for the construction and operation of the LHC, the CMS detector, and the supporting computing infrastructure provided by the following funding agencies: BMBWF and FWF (Austria); FNRS and FWO (Belgium); CNPq, CAPES, FAPERJ, FAPERGS, and FAPESP (Brazil); MES and BNSF (Bulgaria); CERN; CAS, MoST, and NSFC (China); MINCIENCIAS (Colombia); MSES and CSF (Croatia); RIF (Cyprus); SENESCYT (Ecuador); MoER, ERC PUT and ERDF (Estonia); Academy of Finland, MEC, and HIP (Finland); CEA and CNRS/IN2P3 (France); BMBF, DFG, and HGF (Germany); GSRI (Greece); NKFIH (Hungary); DAE and DST (India); IPM (Iran); SFI (Ireland); INFN (Italy); MSIP and NRF (Republic of Korea); MES (Latvia); LAS (Lithuania); MOE and UM (Malaysia); BUAP, CINVESTAV, CONACYT, LNS, SEP, and UASLP-FAI (Mexico); MOS (Montenegro); MBIE (New Zealand); PAEC (Pakistan); MES and NSC (Poland); FCT (Portugal);MESTD (Serbia); MCIN/AEI and PCTI (Spain); MOSTR (Sri Lanka); Swiss Funding Agencies (Switzerland); MST (Taipei); MHESI and NSTDA (Thailand); TUBITAK and TENMAK (Turkey); NASU (Ukraine); STFC (United Kingdom); DOE and NSF (USA).

Individuals have received support from the Marie-Curie programme and the European Research Council and Horizon 2020 Grant, contract Nos. 675440, 724704, 752730, 758316, 765710, 824093, 884104, and COST Action CA16108 (European Union); the Leventis Foundation; the Alfred P. Sloan Foundation; the Alexander von Humboldt Foundation; the Belgian Federal Science Policy Office; the Fonds pour la Formation à la Recherche dans l'Industrie et dans l'Agriculture (FRIA-Belgium); the Agentschap voor Innovatie door Wetenschap en Technologie (IWT-Belgium); the F.R.S.-FNRS and FWO (Belgium) under the "Excellence of Science – EOS" – be.h project n. 30820817; the Beijing Municipal Science & Technology Commission, No. Z191100007219010; the Ministry of Education, Youth and Sports (MEYS) of the Czech Republic; the Hellenic Foundation for Research and Innovation (HFRI), Project Number 2288 (Greece); the Deutsche Forschungsgemeinschaft (DFG), under Germany's Excellence Strategy – EXC 2121 "Quantum Universe" – 390833306, and under project number 400140256 - GRK2497; the Hungarian Academy of Sciences, the New National Excellence Program - ÚNKP, the NKFIH research grants K 124845, K 124850, K 128713, K 128786, K 129058, K 131991, K 133046, K 138136, K 143460, K 143477, 2020-2.2.1-ED-2021-00181, and TKP2021-NKTA-64 (Hungary); the Council of Science and Industrial Research, India; the Latvian Council of Science; the Ministry of Education and Science, project no. 2022/WK/14, and the National Science Center, contracts Opus 2021/41/B/ST2/01369 and 2021/43/B/ST2/01552 (Poland); the Fundação para a Ciência e a Tecnologia, grant CEECIND/01334/2018 (Portugal); the National Priorities Research Program by Qatar National Research Fund; MCIN/AEI/10.13039/501100011033,

JHEP07(2023)046

ERDF "a way of making Europe", and the Programa Estatal de Fomento de la Investigación Científica y Técnica de Excelencia María de Maeztu, grant MDM-2017-0765 and Programa Severo Ochoa del Principado de Asturias (Spain); the Chulalongkorn Academic into Its 2nd Century Project Advancement Project, and the National Science, Research and Innovation Fund via the Program Management Unit for Human Resources & Institutional Development, Research and Innovation, grant B05F650021 (Thailand); the Kavli Foundation; the Nvidia Corporation; the SuperMicro Corporation; the Welch Foundation, contract C-1845; and the Weston Havens Foundation (USA).

References

[1] D0 collaboration, *Observation of single top quark production*, *Phys. Rev. Lett.* **103** (2009) 092001 [arXiv:0903.0850] [INSPIRE].

[2] CDF collaboration, *First observation of electroweak single top quark production*, *Phys. Rev. Lett.* **103** (2009) 092002 [arXiv:0903.0885] [INSPIRE].

[3] S. Frixione et al., *Single-top hadroproduction in association with a W boson*, *JHEP* **07** (2008) 029 [arXiv:0805.3067] [INSPIRE].

[4] A.S. Belyaev, E.E. Boos and L.V. Dudko, *Single top quark at future hadron colliders: complete signal and background study*, *Phys. Rev. D* **59** (1999) 075001 [hep-ph/9806332] [INSPIRE].

[5] C.D. White, S. Frixione, E. Laenen and F. Maltoni, *Isolating Wt production at the LHC*, *JHEP* **11** (2009) 074 [arXiv:0908.0631] [INSPIRE].

[6] T.M.P. Tait and C.-P. Yuan, *Single top quark production as a window to physics beyond the standard model*, *Phys. Rev. D* **63** (2000) 014018 [hep-ph/0007298] [INSPIRE].

[7] Q.-H. Cao, J. Wudka and C.-P. Yuan, *Search for new physics via single top production at the LHC*, *Phys. Lett. B* **658** (2007) 50 [arXiv:0704.2809] [INSPIRE].

[8] V. Barger, M. McCaskey and G. Shaughnessy, *Single top and Higgs associated production at the LHC*, *Phys. Rev. D* **81** (2010) 034020 [arXiv:0911.1556] [INSPIRE].

[9] ATLAS collaboration, *Search for dark matter produced in association with bottom or top quarks in $\sqrt{s} = 13$ TeV pp collisions with the ATLAS detector*, *Eur. Phys. J. C* **78** (2018) 18 [arXiv:1710.11412] [INSPIRE].

[10] CMS collaboration, *Search for dark matter produced in association with a single top quark or a top quark pair in proton-proton collisions at $\sqrt{s} = 13$ TeV*, *JHEP* **03** (2019) 141 [arXiv:1901.01553] [INSPIRE].

[11] D. Pinna, A. Zucchetta, M.R. Buckley and F. Canelli, *Single top quarks and dark matter*, *Phys. Rev. D* **96** (2017) 035031 [arXiv:1701.05195] [INSPIRE].

[12] N. Kidonakis, *Theoretical results for electroweak-boson and single-top production*, *PoS* **DIS2015** (2015) 170 [arXiv:1506.04072] [INSPIRE].

[13] ATLAS collaboration, *Evidence for the associated production of a W boson and a top quark in ATLAS at* $\sqrt{s} = 7$ TeV, *Phys. Lett. B* **716** (2012) 142 [arXiv:1205.5764] [INSPIRE].

[14] CMS collaboration, *Evidence for Associated Production of a Single Top Quark and W Boson in pp Collisions at* $\sqrt{s} = 7$ *TeV*, *Phys. Rev. Lett.* **110** (2013) 022003 [arXiv:1209.3489] [INSPIRE].

[15] CMS collaboration, *Observation of the associated production of a single top quark and a W boson in pp collisions at* $\sqrt{s} = 8$ TeV, *Phys. Rev. Lett.* **112** (2014) 231802 [arXiv:1401.2942] [INSPIRE].

[16] ATLAS collaboration, *Measurement of the production cross-section of a single top quark in association with a W boson at 8 TeV with the ATLAS experiment*, *JHEP* **01** (2016) 064 [arXiv:1510.03752] [INSPIRE].

[17] ATLAS collaboration, *Measurement of the cross-section for producing a W boson in association with a single top quark in pp collisions at* $\sqrt{s} = 13$ *TeV with ATLAS*, *JHEP* **01** (2018) 063 [arXiv:1612.07231] [INSPIRE].

[18] CMS collaboration, *Measurement of the production cross section for single top quarks in association with W bosons in proton-proton collisions at* $\sqrt{s} = 13$ TeV, *JHEP* **10** (2018) 117 [arXiv:1805.07399] [INSPIRE].

[19] ATLAS collaboration, *Measurement of differential cross-sections of a single top quark produced in association with a W boson at* $\sqrt{s} = 13$ *TeV with ATLAS*, *Eur. Phys. J. C* **78** (2018) 186 [arXiv:1712.01602] [INSPIRE].

[20] ATLAS collaboration, *Probing the quantum interference between singly and doubly resonant top-quark production in pp collisions at* $\sqrt{s} = 13$ *TeV with the ATLAS detector*, *Phys. Rev. Lett.* **121** (2018) 152002 [arXiv:1806.04667] [INSPIRE].

[21] CMS collaboration, *Observation of tW production in the single-lepton channel in pp collisions at* $\sqrt{s} = 13$ *TeV*, *JHEP* **11** (2021) 111 [arXiv:2109.01706] [INSPIRE].

[22] ATLAS collaboration, *Measurement of single top-quark production in association with a W boson in the single-lepton channel at* $\sqrt{s} = 8$ *TeV with the ATLAS detector*, *Eur. Phys. J. C* **81** (2021) 720 [arXiv:2007.01554] [INSPIRE].

[23] CMS collaboration, *Measurement of inclusive and differential cross sections for single top quark production in association with a W boson in proton-proton collisions at* $\sqrt{s} = 13$ *TeV*, https://www.hepdata.net/record/ins2129461 [DOI:10.17182/HEPDATA.128942].

[24] CMS collaboration, *The CMS Experiment at the CERN LHC*, 2008 *JINST* **3** S08004 [INSPIRE].

[25] CMS collaboration, *Performance of the CMS Level-1 trigger in proton-proton collisions at* $\sqrt{s} = 13$ *TeV*, 2020 *JINST* **15** P10017 [arXiv:2006.10165] [INSPIRE].

[26] CMS collaboration, *The CMS trigger system*, 2017 *JINST* **12** P01020 [arXiv:1609.02366] [INSPIRE].

[27] S. Alioli, P. Nason, C. Oleari and E. Re, *A general framework for implementing NLO calculations in shower Monte Carlo programs: the POWHEG BOX*, *JHEP* **06** (2010) 043 [arXiv:1002.2581] [INSPIRE].

[28] S. Frixione, P. Nason and C. Oleari, *Matching NLO QCD computations with Parton Shower simulations: the POWHEG method*, *JHEP* **11** (2007) 070 [arXiv:0709.2092] [INSPIRE].

JHEP07(2023)046

[29] P. Nason, *A New method for combining NLO QCD with shower Monte Carlo algorithms*, *JHEP* **11** (2004) 040 [hep-ph/0409146] [INSPIRE].

[30] T.M.P. Tait, *The tW^- mode of single top production*, *Phys. Rev. D* **61** (1999) 034001 [hep-ph/9909352] [INSPIRE].

[31] J. Alwall et al., *The automated computation of tree-level and next-to-leading order differential cross sections, and their matching to parton shower simulations*, *JHEP* **07** (2014) 079 [arXiv:1405.0301] [INSPIRE].

[32] F. Demartin et al., *tWH associated production at the LHC*, *Eur. Phys. J. C* **77** (2017) 34 [arXiv:1607.05862] [INSPIRE].

[33] NNPDF collaboration, *Parton distributions from high-precision collider data*, *Eur. Phys. J. C* **77** (2017) 663 [arXiv:1706.00428] [INSPIRE].

[34] NNPDF collaboration, *Parton distributions for the LHC Run II*, *JHEP* **04** (2015) 040 [arXiv:1410.8849] [INSPIRE].

[35] T. Sjöstrand et al., *An introduction to PYTHIA 8.2*, *Comput. Phys. Commun.* **191** (2015) 159 [arXiv:1410.3012] [INSPIRE].

[36] CMS collaboration, *Extraction and validation of a new set of CMS PYTHIA8 tunes from underlying-event measurements*, *Eur. Phys. J. C* **80** (2020) 4 [arXiv:1903.12179] [INSPIRE].

[37] CMS collaboration, *Event generator tunes obtained from underlying event and multiparton scattering measurements*, *Eur. Phys. J. C* **76** (2016) 155 [arXiv:1512.00815] [INSPIRE].

[38] M. Bahr et al., *Herwig++ Physics and Manual*, *Eur. Phys. J. C* **58** (2008) 639 [arXiv:0803.0883] [INSPIRE].

[39] J. Bellm et al., *Herwig 7.0/Herwig++ 3.0 release note*, *Eur. Phys. J. C* **76** (2016) 196 [arXiv:1512.01178] [INSPIRE].

[40] J. Bellm et al., *Herwig 7.1 Release Note*, arXiv:1705.06919 [INSPIRE].

[41] S. Gieseke, C. Rohr and A. Siodmok, *Colour reconnections in Herwig++*, *Eur. Phys. J. C* **72** (2012) 2225 [arXiv:1206.0041] [INSPIRE].

[42] CMS collaboration, *Development and validation of HERWIG 7 tunes from CMS underlying-event measurements*, *Eur. Phys. J. C* **81** (2021) 312 [arXiv:2011.03422] [INSPIRE].

[43] J. Alwall et al., *Comparative study of various algorithms for the merging of parton showers and matrix elements in hadronic collisions*, *Eur. Phys. J. C* **53** (2008) 473 [arXiv:0706.2569] [INSPIRE].

[44] R. Frederix and S. Frixione, *Merging meets matching in MC@NLO*, *JHEP* **12** (2012) 061 [arXiv:1209.6215] [INSPIRE].

[45] GEANT4 collaboration, *GEANT4 — a simulation toolkit*, *Nucl. Instrum. Meth. A* **506** (2003) 250 [INSPIRE].

[46] Y. Li and F. Petriello, *Combining QCD and electroweak corrections to dilepton production in FEWZ*, *Phys. Rev. D* **86** (2012) 094034 [arXiv:1208.5967] [INSPIRE].

[47] J.M. Campbell, R.K. Ellis and C. Williams, *Vector boson pair production at the LHC*, *JHEP* **07** (2011) 018 [arXiv:1105.0020] [INSPIRE].

[48] M. Czakon, P. Fiedler and A. Mitov, *Total top-quark pair-production cross section at hadron colliders through $O(\alpha_S^4)$*, Phys. Rev. Lett. **110** (2013) 252004 [arXiv:1303.6254] [INSPIRE].

[49] M. Czakon and A. Mitov, *Top++: a program for the calculation of the top-pair cross-section at hadron colliders*, Comput. Phys. Commun. **185** (2014) 2930 [arXiv:1112.5675] [INSPIRE].

[50] CMS collaboration, *Measurement of the inelastic proton-proton cross section at $\sqrt{s} = 13$ TeV*, JHEP **07** (2018) 161 [arXiv:1802.02613] [INSPIRE].

[51] CMS collaboration, *Particle-flow reconstruction and global event description with the CMS detector*, 2017 JINST **12** P10003 [arXiv:1706.04965] [INSPIRE].

[52] D. Contardo et al., *Technical Proposal for the Phase-II Upgrade of the CMS Detector*, CERN-LHCC-2015-010 (2015) [DOI:10.17181/CERN.VU8I.D59J].

[53] CMS collaboration, *Performance of electron reconstruction and selection with the CMS detector in proton-proton collisions at $\sqrt{s} = 8$ TeV*, 2015 JINST **10** P06005 [arXiv:1502.02701] [INSPIRE].

[54] CMS collaboration, *Performance of the CMS muon detector and muon reconstruction with proton-proton collisions at $\sqrt{s} =$ 13 TeV*, 2018 JINST **13** P06015 [arXiv:1804.04528] [INSPIRE].

[55] M. Cacciari, G.P. Salam and G. Soyez, *The anti-k_t jet clustering algorithm*, JHEP **04** (2008) 063 [arXiv:0802.1189] [INSPIRE].

[56] M. Cacciari, G.P. Salam and G. Soyez, *FastJet user manual*, Eur. Phys. J. C **72** (2012) 1896 [arXiv:1111.6097] [INSPIRE].

[57] CMS collaboration, *Jet energy scale and resolution in the CMS experiment in pp collisions at 8 TeV*, 2017 JINST **12** P02014 [arXiv:1607.03663] [INSPIRE].

[58] CMS collaboration, *Performance of missing transverse momentum reconstruction in proton-proton collisions at $\sqrt{s} = 13$ TeV using the CMS detector*, 2019 JINST **14** P07004 [arXiv:1903.06078] [INSPIRE].

[59] CMS collaboration, *Performance of the DeepJet b tagging algorithm using 41.9/fb of data from proton-proton collisions at 13 TeV with Phase 1 CMS detector*, CMS-DP-2018-058 (2018).

[60] E. Bols et al., *Jet flavour classification using deepjet*, 2020 JINST **15** P12012 [arXiv:2008.10519] [INSPIRE].

[61] Y. Freund and R.E. Schapire, *A decision-theoretic generalization of on-line learning and an application to boosting*, J. Comput. Syst. Sci. **55** (1997) 119 [arXiv:1997.1504] [INSPIRE].

[62] H. Voss, A. Hocker, J. Stelzer and F. Tegenfeldt, *TMVA, the Toolkit for Multivariate Data Analysis with ROOT*, PoS **ACAT** (2007) 040 [physics/0703039] [INSPIRE].

[63] L. Breiman, J. Friedman, C.J. Stone and R.A. Olshen, *Classification and regression trees*, Chapman and Hall (1984).

[64] L. Moneta et al., *The RooStats project*, PoS **ACAT2010** (2010) 057 [arXiv:1009.1003] [INSPIRE].

[65] R.J. Barlow and C. Beeston, *Fitting using finite Monte Carlo samples*, Comput. Phys. Commun. **77** (1993) 219 [INSPIRE].

JHEP07(2023)046

[66] J.S. Conway, *Incorporating Nuisance Parameters in Likelihoods for Multisource Spectra*, in the proceedings of the *PHYSTAT 2011*, Geneva, Switzerland, January 17–20 (2011), p. 115–120 [DOI:10.5170/CERN-2011-006.115] [arXiv:1103.0354] [INSPIRE].

[67] TheATLAS et al. collaborations, *Procedure for the LHC Higgs boson search combination in Summer 2011*, CMS-NOTE-2011-005, CERN, Geneva (2011).

[68] CMS collaboration, *Object definitions for top quark analyses at the particle level*, CMS-NOTE-2017-004, CERN, Geneva (2017).

[69] CMS collaboration, *Performance of Photon Reconstruction and Identification with the CMS Detector in Proton-Proton Collisions at* $\sqrt{s} = 8$ *TeV*, 2015 *JINST* **10** P08010 [arXiv:1502.02702] [INSPIRE].

[70] CMS collaboration, *Description and performance of track and primary-vertex reconstruction with the CMS tracker*, 2014 *JINST* **9** P10009 [arXiv:1405.6569] [INSPIRE].

[71] CMS collaboration, *Identification of heavy-flavour jets with the CMS detector in pp collisions at* 13 *TeV*, 2018 *JINST* **13** P05011 [arXiv:1712.07158] [INSPIRE].

[72] CMS collaboration, *Measurements of Inclusive W and Z Cross Sections in pp Collisions at* $\sqrt{s} = 7$ *TeV*, *JHEP* **01** (2011) 080 [arXiv:1012.2466] [INSPIRE].

[73] ATLAS collaboration, *Measurement of the Inelastic Proton-Proton Cross Section at* $\sqrt{s} = 13$ *TeV with the ATLAS Detector at the LHC*, *Phys. Rev. Lett.* **117** (2016) 182002 [arXiv:1606.02625] [INSPIRE].

[74] CMS collaboration, *Precision luminosity measurement in proton-proton collisions at* $\sqrt{s} = 13$ *TeV in 2015 and 2016 at CMS*, *Eur. Phys. J. C* **81** (2021) 800 [arXiv:2104.01927] [INSPIRE].

[75] CMS collaboration, *CMS luminosity measurement for the 2017 data-taking period at* $\sqrt{s} = 13$ *TeV*, CMS-PAS-LUM-17-004, CERN, Geneva (2018).

[76] CMS collaboration, *CMS luminosity measurement for the 2018 data-taking period at* $\sqrt{s} = 13$ *TeV*, CMS-PAS-LUM-18-002, CERN, Geneva (2019).

[77] P. Skands, S. Carrazza and J. Rojo, *Tuning PYTHIA 8.1: the Monash 2013 Tune*, *Eur. Phys. J. C* **74** (2014) 3024 [arXiv:1404.5630] [INSPIRE].

[78] CMS collaboration, *Investigations of the impact of the parton shower tuning in Pythia 8 in the modelling of* $t\bar{t}$ *at* $\sqrt{s} = 8$ *and* 13 *TeV*, CMS-PAS-TOP-16-021, CERN, Geneva (2016).

[79] S. Argyropoulos and T. Sjöstrand, *Effects of color reconnection on* $t\bar{t}$ *final states at the LHC*, *JHEP* **11** (2014) 043 [arXiv:1407.6653] [INSPIRE].

[80] CMS collaboration, *CMS PYTHIA 8 colour reconnection tunes based on underlying-event data*, arXiv:2205.02905 [INSPIRE].

[81] CMS collaboration, *Measurement of the top quark mass using proton-proton data at* $\sqrt{(s)} = 7$ *and 8 TeV*, *Phys. Rev. D* **93** (2016) 072004 [arXiv:1509.04044] [INSPIRE].

[82] CMS collaboration, *Measurement of differential cross sections for top quark pair production using the lepton+jets final state in proton-proton collisions at* 13 *TeV*, *Phys. Rev. D* **95** (2017) 092001 [arXiv:1610.04191] [INSPIRE].

[83] CMS collaboration, *Measurement of the differential cross section for top quark pair production in pp collisions at* $\sqrt{s} = 8$ *TeV*, *Eur. Phys. J. C* **75** (2015) 542 [arXiv:1505.04480] [INSPIRE].

JHEP07(2023)046

[84] CMS collaboration, *Measurement of the $t\bar{t}$ production cross section in the all-jets final state in pp collisions at $\sqrt{s} = 8$ TeV*, Eur. Phys. J. C **76** (2016) 128 [arXiv:1509.06076] [INSPIRE].

[85] CMS collaboration, *Measurement of the $t\bar{t}$ production cross section, the top quark mass, and the strong coupling constant using dilepton events in pp collisions at $\sqrt{s} = 13$ TeV*, Eur. Phys. J. C **79** (2019) 368 [arXiv:1812.10505] [INSPIRE].

[86] CMS collaboration, *Measurement of differential $t\bar{t}$ production cross sections in the full kinematic range using lepton+jets events from proton-proton collisions at $\sqrt{s} = 13$ TeV*, Phys. Rev. D **104** (2021) 092013 [arXiv:2108.02803] [INSPIRE].

[87] CMS collaboration, *Measurement of the top quark polarization and $t\bar{t}$ spin correlations using dilepton final states in proton-proton collisions at $\sqrt{s} = 13$ TeV*, Phys. Rev. D **100** (2019) 072002 [arXiv:1907.03729] [INSPIRE].

JHEP07(2023)046

The CMS collaboration

Yerevan Physics Institute, Yerevan, Armenia
A. Tumasyan[1]

Institut für Hochenergiephysik, Vienna, Austria
W. Adam, J.W. Andrejkovic, T. Bergauer, S. Chatterjee, K. Damanakis, M. Dragicevic, A. Escalante Del Valle, P.S. Hussain, M. Jeitler[2], N. Krammer, L. Lechner, D. Liko, I. Mikulec, P. Paulitsch, F.M. Pitters, J. Schieck[2], R. Schöfbeck, D. Schwarz, S. Templ, W. Waltenberger, C.-E. Wulz[2]

Universiteit Antwerpen, Antwerpen, Belgium
M.R. Darwish[3], T. Janssen, T. Kello[4], H. Rejeb Sfar, P. Van Mechelen

Vrije Universiteit Brussel, Brussel, Belgium
E.S. Bols, J. D'Hondt, A. De Moor, M. Delcourt, H. El Faham, S. Lowette, S. Moortgat, A. Morton, D. Müller, A.R. Sahasransu, S. Tavernier, W. Van Doninck, D. Vannerom

Université Libre de Bruxelles, Bruxelles, Belgium
B. Clerbaux, G. De Lentdecker, L. Favart, D. Hohov, J. Jaramillo, K. Lee, M. Mahdavikhorrami, I. Makarenko, A. Malara, S. Paredes, L. Pétré, N. Postiau, L. Thomas, M. Vanden Bemden, C. Vander Velde, P. Vanlaer

Ghent University, Ghent, Belgium
D. Dobur, J. Knolle, L. Lambrecht, G. Mestdach, M. Niedziela, C. Rendón, C. Roskas, A. Samalan, K. Skovpen, M. Tytgat, N. Van Den Bossche, B. Vermassen, L. Wezenbeek

Université Catholique de Louvain, Louvain-la-Neuve, Belgium
A. Benecke, G. Bruno, F. Bury, C. Caputo, P. David, C. Delaere, I.S. Donertas, A. Giammanco, K. Jaffel, Sa. Jain, V. Lemaitre, K. Mondal, A. Taliercio, T.T. Tran, P. Vischia, S. Wertz

Centro Brasileiro de Pesquisas Fisicas, Rio de Janeiro, Brazil
G.A. Alves, E. Coelho, C. Hensel, A. Moraes, P. Rebello Teles

Universidade do Estado do Rio de Janeiro, Rio de Janeiro, Brazil
W.L. Aldá Júnior, M. Alves Gallo Pereira, M. Barroso Ferreira Filho, H. Brandao Malbouisson, W. Carvalho, J. Chinellato[5], E.M. Da Costa, G.G. Da Silveira[6], D. De Jesus Damiao, V. Dos Santos Sousa, S. Fonseca De Souza, J. Martins[7], C. Mora Herrera, K. Mota Amarilo, L. Mundim, H. Nogima, A. Santoro, S.M. Silva Do Amaral, A. Sznajder, M. Thiel, F. Torres Da Silva De Araujo[8], A. Vilela Pereira

JHEP07(2023)046

Universidade Estadual Paulista, Universidade Federal do ABC, São Paulo, Brazil
C.A. Bernardes[6], L. Calligaris, T.R. Fernandez Perez Tomei, E.M. Gregores, P.G. Mercadante, S.F. Novaes, Sandra S. Padula

Institute for Nuclear Research and Nuclear Energy, Bulgarian Academy of Sciences, Sofia, Bulgaria
A. Aleksandrov, G. Antchev, R. Hadjiiska, P. Iaydjiev, M. Misheva, M. Rodozov, M. Shopova, G. Sultanov

University of Sofia, Sofia, Bulgaria
A. Dimitrov, T. Ivanov, L. Litov, B. Pavlov, P. Petkov, A. Petrov, E. Shumka

Instituto De Alta Investigación, Universidad de Tarapacá, Casilla 7 D, Arica, Chile
S.Thakur

Beihang University, Beijing, China
T. Cheng, T. Javaid[9], M. Mittal, L. Yuan

Department of Physics, Tsinghua University, Beijing, China
M. Ahmad, G. Bauer[10], Z. Hu, S. Lezki, K. Yi[10,11]

Institute of High Energy Physics, Beijing, China
G.M. Chen[9], H.S. Chen[9], M. Chen[9], F. Iemmi, C.H. Jiang, A. Kapoor, H. Kou, H. Liao, Z.-A. Liu[12], V. Milosevic, F. Monti, R. Sharma, J. Tao, J. Thomas-Wilsker, J. Wang, H. Zhang, J. Zhao

State Key Laboratory of Nuclear Physics and Technology, Peking University, Beijing, China
A. Agapitos, Y. An, Y. Ban, C. Chen, A. Levin, C. Li, Q. Li, X. Lyu, Y. Mao, S.J. Qian, X. Sun, D. Wang, J. Xiao, H. Yang

Sun Yat-Sen University, Guangzhou, China
M. Lu, Z. You

Institute of Modern Physics and Key Laboratory of Nuclear Physics and Ion-beam Application (MOE) - Fudan University, Shanghai, China
X. Gao[4], D. Leggat, H. Okawa, Y. Zhang

Zhejiang University, Hangzhou, Zhejiang, China
Z. Lin, C. Lu, M. Xiao

Universidad de Los Andes, Bogota, Colombia
C. Avila, D.A. Barbosa Trujillo, A. Cabrera, C. Florez, J. Fraga

Universidad de Antioquia, Medellin, Colombia
J. Mejia Guisao, F. Ramirez, M. Rodriguez, J.D. Ruiz Alvarez

University of Split, Faculty of Electrical Engineering, Mechanical Engineering and Naval Architecture, Split, Croatia
D. Giljanovic, N. Godinovic, D. Lelas, I. Puljak

University of Split, Faculty of Science, Split, Croatia
Z. Antunovic, M. Kovac, T. Sculac

Institute Rudjer Boskovic, Zagreb, Croatia
V. Brigljevic, B.K. Chitroda, D. Ferencek, D. Majumder, S. Mishra, M. Roguljic, A. Starodumov[13], T. Susa

University of Cyprus, Nicosia, Cyprus
A. Attikis, K. Christoforou, M. Kolosova, S. Konstantinou, J. Mousa, C. Nicolaou, F. Ptochos, P.A. Razis, H. Rykaczewski, H. Saka, A. Stepennov

Charles University, Prague, Czech Republic
M. Finger[13], M. Finger Jr.[13], A. Kveton

Escuela Politecnica Nacional, Quito, Ecuador
E. Ayala

Universidad San Francisco de Quito, Quito, Ecuador
E. Carrera Jarrin

Academy of Scientific Research and Technology of the Arab Republic of Egypt, Egyptian Network of High Energy Physics, Cairo, Egypt
H. Abdalla[14], Y. Assran[15,16]

Center for High Energy Physics (CHEP-FU), Fayoum University, El-Fayoum, Egypt
M.A. Mahmoud, Y. Mohammed

National Institute of Chemical Physics and Biophysics, Tallinn, Estonia
S. Bhowmik, R.K. Dewanjee, K. Ehataht, M. Kadastik, T. Lange, S. Nandan, C. Nielsen, J. Pata, M. Raidal, L. Tani, C. Veelken

Department of Physics, University of Helsinki, Helsinki, Finland
P. Eerola, H. Kirschenmann, K. Osterberg, M. Voutilainen

Helsinki Institute of Physics, Helsinki, Finland
S. Bharthuar, E. Brücken, F. Garcia, J. Havukainen, M.S. Kim, R. Kinnunen, T. Lampén, K. Lassila-Perini, S. Lehti, T. Lindén, M. Lotti, L. Martikainen, M. Myllymäki, J. Ott, M.m. Rantanen, H. Siikonen, E. Tuominen, J. Tuominiemi

Lappeenranta-Lahti University of Technology, Lappeenranta, Finland
P. Luukka, H. Petrow, T. Tuuva

IRFU, CEA, Université Paris-Saclay, Gif-sur-Yvette, France
C. Amendola, M. Besancon, F. Couderc, M. Dejardin, D. Denegri, J.L. Faure, F. Ferri, S. Ganjour, P. Gras, G. Hamel de Monchenault, P. Jarry, V. Lohezic, J. Malcles, J. Rander, A. Rosowsky, M.Ö. Sahin, A. Savoy-Navarro[17], P. Simkina, M. Titov

Laboratoire Leprince-Ringuet, CNRS/IN2P3, Ecole Polytechnique, Institut Polytechnique de Paris, Palaiseau, France
C. Baldenegro Barrera, F. Beaudette, A. Buchot Perraguin, P. Busson, A. Cappati, C. Charlot, F. Damas, O. Davignon, B. Diab, G. Falmagne, B.A. Fontana Santos Alves, S. Ghosh, R. Granier de Cassagnac, A. Hakimi, B. Harikrishnan, G. Liu, J. Motta, M. Nguyen, C. Ochando, L. Portales, R. Salerno, U. Sarkar, J.B. Sauvan, Y. Sirois, A. Tarabini, E. Vernazza, A. Zabi, A. Zghiche

Université de Strasbourg, CNRS, IPHC UMR 7178, Strasbourg, France
J.-L. Agram[18], J. Andrea, D. Apparu, D. Bloch, G. Bourgatte, J.-M. Brom, E.C. Chabert, C. Collard, D. Darej, U. Goerlach, C. Grimault, A.-C. Le Bihan, P. Van Hove

Institut de Physique des 2 Infinis de Lyon (IP2I), Villeurbanne, France
S. Beauceron, B. Blancon, G. Boudoul, A. Carle, N. Chanon, J. Choi, D. Contardo, P. Depasse, C. Dozen[19], H. El Mamouni, J. Fay, S. Gascon, M. Gouzevitch, G. Grenier, B. Ille, I.B. Laktineh, M. Lethuillier, L. Mirabito, S. Perries, L. Torterotot, M. Vander Donckt, P. Verdier, S. Viret

Georgian Technical University, Tbilisi, Georgia
D. Chokheli, I. Lomidze, Z. Tsamalaidze[13]

RWTH Aachen University, I. Physikalisches Institut, Aachen, Germany
V. Botta, L. Feld, K. Klein, M. Lipinski, D. Meuser, A. Pauls, N. Röwert, M. Teroerde

RWTH Aachen University, III. Physikalisches Institut A, Aachen, Germany
S. Diekmann, A. Dodonova, N. Eich, D. Eliseev, M. Erdmann, P. Fackeldey, D. Fasanella, B. Fischer, T. Hebbeker, K. Hoepfner, F. Ivone, M.y. Lee, L. Mastrolorenzo, M. Merschmeyer, A. Meyer, S. Mondal, S. Mukherjee, D. Noll, A. Novak, F. Nowotny, A. Pozdnyakov, Y. Rath, W. Redjeb, H. Reithler, A. Schmidt, S.C. Schuler, A. Sharma, L. Vigilante, S. Wiedenbeck, S. Zaleski

RWTH Aachen University, III. Physikalisches Institut B, Aachen, Germany
C. Dziwok, G. Flügge, W. Haj Ahmad[20], O. Hlushchenko, T. Kress, A. Nowack, O. Pooth, A. Stahl, T. Ziemons, A. Zotz

JHEP07(2023)046

Deutsches Elektronen-Synchrotron, Hamburg, Germany

H. Aarup Petersen, M. Aldaya Martin, P. Asmuss, S. Baxter, M. Bayatmakou, O. Behnke, A. Bermúdez Martínez, S. Bhattacharya, A.A. Bin Anuar, F. Blekman[21], K. Borras[22], D. Brunner, A. Campbell, A. Cardini, C. Cheng, F. Colombina, S. Consuegra Rodríguez, G. Correia Silva, M. De Silva, L. Didukh, G. Eckerlin, D. Eckstein, L.I. Estevez Banos, O. Filatov, E. Gallo[21], A. Geiser, A. Giraldi, G. Greau, A. Grohsjean, V. Guglielmi, M. Guthoff, A. Jafari[23], N.Z. Jomhari, B. Kaech, A. Kasem[22], M. Kasemann, H. Kaveh, C. Kleinwort, R. Kogler, M. Komm, D. Krücker, W. Lange, D. Leyva Pernia, K. Lipka[24], W. Lohmann[25], R. Mankel, I.-A. Melzer-Pellmann, M. Mendizabal Morentin, J. Metwally, A.B. Meyer, G. Milella, M. Mormile, A. Mussgiller, A. Nürnberg, Y. Otarid, D. Pérez Adán, A. Raspereza, B. Ribeiro Lopes, J. Rübenach, A. Saggio, A. Saibel, M. Savitskyi, M. Scham[26,22], V. Scheurer, S. Schnake[22], P. Schütze, C. Schwanenberger[21], M. Shchedrolosiev, R.E. Sosa Ricardo, D. Stafford, N. Tonon[†], M. Van De Klundert, F. Vazzoler, A. Ventura Barroso, R. Walsh, D. Walter, Q. Wang, Y. Wen, K. Wichmann, L. Wiens[22], C. Wissing, S. Wuchterl, Y. Yang, A. Zimermmane Castro Santos

University of Hamburg, Hamburg, Germany

A. Albrecht, S. Albrecht, M. Antonello, S. Bein, L. Benato, M. Bonanomi, P. Connor, K. De Leo, M. Eich, K. El Morabit, F. Feindt, A. Fröhlich, C. Garbers, E. Garutti, M. Hajheidari, J. Haller, A. Hinzmann, H.R. Jabusch, G. Kasieczka, P. Keicher, R. Klanner, W. Korcari, T. Kramer, V. Kutzner, F. Labe, J. Lange, A. Lobanov, C. Matthies, A. Mehta, L. Moureaux, M. Mrowietz, A. Nigamova, Y. Nissan, A. Paasch, K.J. Pena Rodriguez, T. Quadfasel, M. Rieger, O. Rieger, D. Savoiu, P. Schleper, M. Schröder, J. Schwandt, M. Sommerhalder, H. Stadie, G. Steinbrück, A. Tews, M. Wolf

Karlsruher Institut fuer Technologie, Karlsruhe, Germany

S. Brommer, M. Burkart, E. Butz, R. Caspart, T. Chwalek, A. Dierlamm, A. Droll, N. Faltermann, M. Giffels, J.O. Gosewisch, A. Gottmann, F. Hartmann[27], M. Horzela, U. Husemann, M. Klute, R. Koppenhöfer, S. Maier, S. Mitra, Th. Müller, M. Neukum, M. Oh, G. Quast, K. Rabbertz, J. Rauser, M. Schnepf, D. Seith, I. Shvetsov, H.J. Simonis, N. Trevisani, R. Ulrich, J. van der Linden, R.F. Von Cube, M. Wassmer, S. Wieland, R. Wolf, S. Wozniewski, S. Wunsch, X. Zuo

Institute of Nuclear and Particle Physics (INPP), NCSR Demokritos, Aghia Paraskevi, Greece

G. Anagnostou, P. Assiouras, G. Daskalakis, A. Kyriakis, A. Stakia

National and Kapodistrian University of Athens, Athens, Greece

M. Diamantopoulou, D. Karasavvas, P. Kontaxakis, A. Manousakis-Katsikakis, A. Panagiotou, I. Papavergou, N. Saoulidou, K. Theofilatos, E. Tziaferi, K. Vellidis, I. Zisopoulos

JHEP07(2023)046

National Technical University of Athens, Athens, Greece
G. Bakas, T. Chatzistavrou, K. Kousouris, I. Papakrivopoulos, G. Tsipolitis, A. Zacharopoulou

University of Ioánnina, Ioánnina, Greece
K. Adamidis, I. Bestintzanos, I. Evangelou, C. Foudas, P. Gianneios, C. Kamtsikis, P. Katsoulis, P. Kokkas, P.G. Kosmoglou Kioseoglou, N. Manthos, I. Papadopoulos, J. Strologas

MTA-ELTE Lendület CMS Particle and Nuclear Physics Group, Eötvös Loránd University, Budapest, Hungary
M. Csanád, K. Farkas, M.M.A. Gadallah[28], S. Lökös[29], P. Major, K. Mandal, G. Pásztor, A.J. Rádl[30], O. Surányi, G.I. Veres

Wigner Research Centre for Physics, Budapest, Hungary
M. Bartók[31], G. Bencze, C. Hajdu, D. Horvath[32,33], F. Sikler, V. Veszpremi

Institute of Nuclear Research ATOMKI, Debrecen, Hungary
N. Beni, S. Czellar, J. Karancsi[31], J. Molnar, Z. Szillasi, D. Teyssier

Institute of Physics, University of Debrecen, Debrecen, Hungary
P. Raics, B. Ujvari[34]

Karoly Robert Campus, MATE Institute of Technology, Gyongyos, Hungary
T. Csorgo[30], F. Nemes[30], T. Novak

Panjab University, Chandigarh, India
J. Babbar, S. Bansal, S.B. Beri, V. Bhatnagar, G. Chaudhary, S. Chauhan, N. Dhingra[35], R. Gupta, A. Kaur, A. Kaur, H. Kaur, M. Kaur, S. Kumar, P. Kumari, M. Meena, K. Sandeep, T. Sheokand, J.B. Singh[36], A. Singla, A. K. Virdi

University of Delhi, Delhi, India
A. Ahmed, A. Bhardwaj, B.C. Choudhary, A. Kumar, M. Naimuddin, K. Ranjan, S. Saumya

Saha Institute of Nuclear Physics, HBNI, Kolkata, India
S. Baradia, S. Barman[37], S. Bhattacharya, D. Bhowmik, S. Dutta, S. Dutta, B. Gomber[38], M. Maity[37], P. Palit, G. Saha, B. Sahu, S. Sarkar

Indian Institute of Technology Madras, Madras, India
P.K. Behera, S.C. Behera, P. Kalbhor, J.R. Komaragiri[39], D. Kumar[39], A. Muhammad, L. Panwar[39], R. Pradhan, P.R. Pujahari, A. Sharma, A.K. Sikdar, P.C. Tiwari[39], S. Verma

Bhabha Atomic Research Centre, Mumbai, India
K. Naskar[40]

JHEP07(2023)046

Tata Institute of Fundamental Research-A, Mumbai, India
T. Aziz, I. Das, S. Dugad, M. Kumar, G.B. Mohanty, P. Suryadevara

Tata Institute of Fundamental Research-B, Mumbai, India
S. Banerjee, R. Chudasama, M. Guchait, S. Karmakar, S. Kumar, G. Majumder, K. Mazumdar, S. Mukherjee, A. Thachayath

National Institute of Science Education and Research, An OCC of Homi Bhabha National Institute, Bhubaneswar, Odisha, India
S. Bahinipati[41], C. Kar, P. Mal, T. Mishra, V.K. Muraleedharan Nair Bindhu[42], A. Nayak[42], P. Saha, S.K. Swain, D. Vats[42]

Indian Institute of Science Education and Research (IISER), Pune, India
A. Alpana, S. Dube, B. Kansal, A. Laha, S. Pandey, A. Rastogi, S. Sharma

Isfahan University of Technology, Isfahan, Iran
H. Bakhshiansohi[43], E. Khazaie, M. Zeinali[44]

Institute for Research in Fundamental Sciences (IPM), Tehran, Iran
S. Chenarani[45], S.M. Etesami, M. Khakzad, M. Mohammadi Najafabadi

University College Dublin, Dublin, Ireland
M. Grunewald

INFN Sezione di Bari[a], Università di Bari[b], Politecnico di Bari[c], Bari, Italy
M. Abbrescia[a,b], R. Aly[a,c,46], C. Aruta[a,b], A. Colaleo[a], D. Creanza[a,c], N. De Filippis[a,c], M. De Palma[a,b], A. Di Florio[a,b], W. Elmetenawee[a,b], F. Errico[a,b], L. Fiore[a], G. Iaselli[a,c], M. Ince[a,b], G. Maggi[a,c], M. Maggi[a], I. Margjeka[a,b], V. Mastrapasqua[a,b], S. My[a,b], S. Nuzzo[a,b], A. Pellecchia[a,b], A. Pompili[a,b], G. Pugliese[a,c], R. Radogna[a], D. Ramos[a], A. Ranieri[a], G. Selvaggi[a,b], L. Silvestris[a], F.M. Simone[a,b], Ü. Sözbilir[a], A. Stamerra[a], R. Venditti[a], P. Verwilligen[a]

INFN Sezione di Bologna[a], Università di Bologna[b], Bologna, Italy
G. Abbiendi[a], C. Battilana[a,b], D. Bonacorsi[a,b], L. Borgonovi[a], L. Brigliadori[a], R. Campanini[a,b], P. Capiluppi[a,b], A. Castro[a,b], F.R. Cavallo[a], M. Cuffiani[a,b], G.M. Dallavalle[a], T. Diotalevi[a,b], F. Fabbri[a], A. Fanfani[a,b], P. Giacomelli[a], L. Giommi[a,b], C. Grandi[a], L. Guiducci[a,b], S. Lo Meo[a,47], L. Lunerti[a,b], S. Marcellini[a], G. Masetti[a], F.L. Navarria[a,b], A. Perrotta[a], F. Primavera[a,b], A.M. Rossi[a,b], T. Rovelli[a,b], G.P. Siroli[a,b]

INFN Sezione di Catania[a], Università di Catania[b], Catania, Italy
S. Costa[a,b,48], A. Di Mattia[a], R. Potenza[a,b], A. Tricomi[a,b,48], C. Tuve[a,b]

INFN Sezione di Firenze[a], Università di Firenze[b], Firenze, Italy
G. Barbagli[a], G. Bardelli[a,b], B. Camaiani[a,b], A. Cassese[a], R. Ceccarelli[a,b], V. Ciulli[a,b], C. Civinini[a], R. D'Alessandro[a,b], E. Focardi[a,b], G. Latino[a,b], P. Lenzi[a,b], M. Lizzo[a,b], M. Meschini[a], S. Paoletti[a], R. Seidita[a,b], G. Sguazzoni[a], L. Viliani[a]

JHEP07(2023)046

INFN Laboratori Nazionali di Frascati, Frascati, Italy

L. Benussi, S. Bianco, S. Meola[27], D. Piccolo

INFN Sezione di Genova[a], Università di Genova[b], Genova, Italy

M. Bozzo[a,b], P. Chatagnon[a], F. Ferro[a], R. Mulargia[a], E. Robutti[a], S. Tosi[a,b]

INFN Sezione di Milano-Bicocca[a], Università di Milano-Bicocca[b], Milano, Italy

A. Benaglia[a], G. Boldrini[a], F. Brivio[a,b], F. Cetorelli[a,b], F. De Guio[a,b], M.E. Dinardo[a,b], P. Dini[a], S. Gennai[a], A. Ghezzi[a,b], P. Govoni[a,b], L. Guzzi[a,b], M.T. Lucchini[a,b], M. Malberti[a], S. Malvezzi[a], A. Massironi[a], D. Menasce[a], L. Moroni[a], M. Paganoni[a,b], D. Pedrini[a], B.S. Pinolini[a], S. Ragazzi[a,b], N. Redaelli[a], T. Tabarelli de Fatis[a,b], D. Zuolo[a,b]

INFN Sezione di Napoli[a], Università di Napoli 'Federico II'[b], Napoli, Italy; Università della Basilicata[c], Potenza, Italy; Università G. Marconi[d], Roma, Italy

S. Buontempo[a], F. Carnevali[a,b], N. Cavallo[a,c], A. De Iorio[a,b], F. Fabozzi[a,c], A.O.M. Iorio[a,b], L. Lista[a,b,49], P. Paolucci[a,27], B. Rossi[a], C. Sciacca[a,b]

INFN Sezione di Padova[a], Università di Padova[b], Padova, Italy; Università di Trento[c], Trento, Italy

P. Azzi[a], N. Bacchetta[a,50], M. Benettoni[a], A. Bergnoli[a], D. Bisello[a,b], P. Bortignon[a], A. Bragagnolo[a,b], R. Carlin[a,b], P. Checchia[a], T. Dorigo[a], F. Gasparini[a,b], U. Gasparini[a,b], G. Grosso[a], L. Layer[a,51], E. Lusiani[a], M. Margoni[a,b], J. Pazzini[a,b], P. Ronchese[a,b], R. Rossin[a,b], G. Strong[a], M. Tosi[a,b], H. Yarar[a,b], M. Zanetti[a,b], P. Zotto[a,b], A. Zucchetta[a,b], G. Zumerle[a,b]

INFN Sezione di Pavia[a], Università di Pavia[b], Pavia, Italy

S. Abu Zeid[a,52], C. Aimè[a,b], A. Braghieri[a], S. Calzaferri[a,b], D. Fiorina[a,b], P. Montagna[a,b], V. Re[a], C. Riccardi[a,b], P. Salvini[a], I. Vai[a], P. Vitulo[a,b]

INFN Sezione di Perugia[a], Università di Perugia[b], Perugia, Italy

P. Asenov[a,53], G.M. Bilei[a], D. Ciangottini[a,b], L. Fanò[a,b], M. Magherini[a,b], G. Mantovani[a,b], V. Mariani[a,b], M. Menichelli[a], F. Moscatelli[a,53], A. Piccinelli[a,b], M. Presilla[a,b], A. Rossi[a,b], A. Santocchia[a,b], D. Spiga[a], T. Tedeschi[a,b]

INFN Sezione di Pisa[a], Università di Pisa[b], Scuola Normale Superiore di Pisa[c], Pisa, Italy; Università di Siena[d], Siena, Italy

P. Azzurri[a], G. Bagliesi[a], V. Bertacchi[a,c], R. Bhattacharya[a], L. Bianchini[a,b], T. Boccali[a], E. Bossini[a,b], D. Bruschini[a,c], R. Castaldi[a], M.A. Ciocci[a,b], V. D'Amante[a,d], R. Dell'Orso[a], M.R. Di Domenico[a,d], S. Donato[a], A. Giassi[a], F. Ligabue[a,c], G. Mandorli[a,c], D. Matos Figueiredo[a], A. Messineo[a,b], M. Musich[a,b], F. Palla[a], S. Parolia[a,b], G. Ramirez-Sanchez[a,c], A. Rizzi[a,b], G. Rolandi[a,c],

S. Roy Chowdhury[a], T. Sarkar[a], A. Scribano[a], N. Shafiei[a,b], P. Spagnolo[a], R. Tenchini[a], G. Tonelli[a,b], N. Turini[a,d], A. Venturi[a], P.G. Verdini[a]

INFN Sezione di Roma[a], Sapienza Università di Roma[b], Roma, Italy
P. Barria[a], M. Campana[a,b], F. Cavallari[a], D. Del Re[a,b], E. Di Marco[a], M. Diemoz[a], E. Longo[a,b], P. Meridiani[a], G. Organtini[a,b], F. Pandolfi[a], R. Paramatti[a,b], C. Quaranta[a,b], S. Rahatlou[a,b], C. Rovelli[a], F. Santanastasio[a,b], L. Soffi[a], R. Tramontano[a,b]

INFN Sezione di Torino[a], Università di Torino[b], Torino, Italy; Università del Piemonte Orientale[c], Novara, Italy
N. Amapane[a,b], R. Arcidiacono[a,c], S. Argiro[a,b], M. Arneodo[a,c], N. Bartosik[a], R. Bellan[a,b], A. Bellora[a,b], C. Biino[a], N. Cartiglia[a], M. Costa[a,b], R. Covarelli[a,b], N. Demaria[a], M. Grippo[a,b], B. Kiani[a,b], F. Legger[a], C. Mariotti[a], S. Maselli[a], A. Mecca[a,b], E. Migliore[a,b], E. Monteil[a,b], M. Monteno[a], M.M. Obertino[a,b], G. Ortona[a], L. Pacher[a,b], N. Pastrone[a], M. Pelliccioni[a], M. Ruspa[a,c], K. Shchelina[a], F. Siviero[a,b], V. Sola[a], A. Solano[a,b], D. Soldi[a,b], A. Staiano[a], M. Tornago[a,b], D. Trocino[a], G. Umoret[a,b], A. Vagnerini[a,b]

INFN Sezione di Trieste[a], Università di Trieste[b], Trieste, Italy
S. Belforte[a], V. Candelise[a,b], M. Casarsa[a], F. Cossutti[a], A. Da Rold[a,b], G. Della Ricca[a,b], G. Sorrentino[a,b]

Kyungpook National University, Daegu, Korea
S. Dogra, C. Huh, B. Kim, D.H. Kim, G.N. Kim, J. Kim, J. Lee, S.W. Lee, C.S. Moon, Y.D. Oh, S.I. Pak, M.S. Ryu, S. Sekmen, Y.C. Yang

Chonnam National University, Institute for Universe and Elementary Particles, Kwangju, Korea
H. Kim, D.H. Moon

Hanyang University, Seoul, Korea
E. Asilar, T.J. Kim, J. Park

Korea University, Seoul, Korea
S. Choi, S. Han, B. Hong, K. Lee, K.S. Lee, J. Lim, J. Park, S.K. Park, J. Yoo

Kyung Hee University, Department of Physics, Seoul, Korea
J. Goh

Sejong University, Seoul, Korea
H. S. Kim, Y. Kim, S. Lee

Seoul National University, Seoul, Korea
J. Almond, J.H. Bhyun, J. Choi, S. Jeon, J. Kim, J.S. Kim, S. Ko, H. Kwon, H. Lee, S. Lee, B.H. Oh, S.B. Oh, H. Seo, U.K. Yang, I. Yoon

JHEP07(2023)046

University of Seoul, Seoul, Korea
W. Jang, D.Y. Kang, Y. Kang, D. Kim, S. Kim, B. Ko, J.S.H. Lee, Y. Lee, J.A. Merlin, I.C. Park, Y. Roh, D. Song, Watson, I.J., S. Yang

Yonsei University, Department of Physics, Seoul, Korea
S. Ha, H.D. Yoo

Sungkyunkwan University, Suwon, Korea
M. Choi, M.R. Kim, H. Lee, Y. Lee, Y. Lee, I. Yu

College of Engineering and Technology, American University of the Middle East (AUM), Dasman, Kuwait
T. Beyrouthy, Y. Maghrbi

Riga Technical University, Riga, Latvia
K. Dreimanis, G. Pikurs, M. Seidel, V. Veckalns

Vilnius University, Vilnius, Lithuania
M. Ambrozas, A. Carvalho Antunes De Oliveira, A. Juodagalvis, A. Rinkevicius, G. Tamulaitis

National Centre for Particle Physics, Universiti Malaya, Kuala Lumpur, Malaysia
N. Bin Norjoharuddeen, S.Y. Hoh[54], I. Yusuff[54], Z. Zolkapli

Universidad de Sonora (UNISON), Hermosillo, Mexico
J.F. Benitez, A. Castaneda Hernandez, H.A. Encinas Acosta, L.G. Gallegos Maríñez, M. León Coello, J.A. Murillo Quijada, A. Sehrawat, L. Valencia Palomo

Centro de Investigacion y de Estudios Avanzados del IPN, Mexico City, Mexico
G. Ayala, H. Castilla-Valdez, I. Heredia-De La Cruz[55], R. Lopez-Fernandez, C.A. Mondragon Herrera, D.A. Perez Navarro, A. Sánchez Hernández

Universidad Iberoamericana, Mexico City, Mexico
C. Oropeza Barrera, F. Vazquez Valencia

Benemerita Universidad Autonoma de Puebla, Puebla, Mexico
I. Pedraza, H.A. Salazar Ibarguen, C. Uribe Estrada

University of Montenegro, Podgorica, Montenegro
I. Bubanja, J. Mijuskovic[56], N. Raicevic

National Centre for Physics, Quaid-I-Azam University, Islamabad, Pakistan
A. Ahmad, M.I. Asghar, A. Awais, M.I.M. Awan, M. Gul, H.R. Hoorani, W.A. Khan, M. Shoaib, M. Waqas

AGH University of Science and Technology Faculty of Computer Science, Electronics and Telecommunications, Krakow, Poland
V. Avati, L. Grzanka, M. Malawski

National Centre for Nuclear Research, Swierk, Poland
H. Bialkowska, M. Bluj, B. Boimska, M. Górski, M. Kazana, M. Szleper, P. Zalewski

Institute of Experimental Physics, Faculty of Physics, University of Warsaw, Warsaw, Poland
K. Bunkowski, K. Doroba, A. Kalinowski, M. Konecki, J. Krolikowski

Laboratório de Instrumentação e Física Experimental de Partículas, Lisboa, Portugal
M. Araujo, P. Bargassa, D. Bastos, A. Boletti, P. Faccioli, M. Gallinaro, J. Hollar, N. Leonardo, T. Niknejad, M. Pisano, J. Seixas, J. Varela

VINCA Institute of Nuclear Sciences, University of Belgrade, Belgrade, Serbia
P. Adzic[57], M. Dordevic, P. Milenovic, J. Milosevic

Centro de Investigaciones Energéticas Medioambientales y Tecnológicas (CIEMAT), Madrid, Spain
M. Aguilar-Benitez, J. Alcaraz Maestre, A. Álvarez Fernández, M. Barrio Luna, Cristina F. Bedoya, C.A. Carrillo Montoya, M. Cepeda, M. Cerrada, N. Colino, B. De La Cruz, A. Delgado Peris, D. Fernández Del Val, J.P. Fernández Ramos, J. Flix, M.C. Fouz, O. Gonzalez Lopez, S. Goy Lopez, J.M. Hernandez, M.I. Josa, J. León Holgado, D. Moran, C. Perez Dengra, A. Pérez-Calero Yzquierdo, J. Puerta Pelayo, I. Redondo, D.D. Redondo Ferrero, L. Romero, S. Sánchez Navas, J. Sastre, L. Urda Gómez, J. Vazquez Escobar, C. Willmott

Universidad Autónoma de Madrid, Madrid, Spain
J.F. de Trocóniz

Universidad de Oviedo, Instituto Universitario de Ciencias y Tecnologías Espaciales de Asturias (ICTEA), Oviedo, Spain
B. Alvarez Gonzalez, J. Cuevas, J. Fernandez Menendez, S. Folgueras, I. Gonzalez Caballero, J.R. González Fernández, E. Palencia Cortezon, C. Ramón Álvarez, V. Rodríguez Bouza, A. Soto Rodríguez, A. Trapote, C. Vico Villalba

Instituto de Física de Cantabria (IFCA), CSIC-Universidad de Cantabria, Santander, Spain
J.A. Brochero Cifuentes, I.J. Cabrillo, A. Calderon, J. Duarte Campderros, M. Fernandez, C. Fernandez Madrazo, A. García Alonso, G. Gomez, C. Lasaosa García,

C. Martinez Rivero, P. Martinez Ruiz del Arbol, F. Matorras, P. Matorras Cuevas, J. Piedra Gomez, C. Prieels, A. Ruiz-Jimeno, L. Scodellaro, I. Vila, J.M. Vizan Garcia

University of Colombo, Colombo, Sri Lanka

M.K. Jayananda, B. Kailasapathy[58], D.U.J. Sonnadara, D.D.C. Wickramarathna

University of Ruhuna, Department of Physics, Matara, Sri Lanka

W.G.D. Dharmaratna, K. Liyanage, N. Perera, N. Wickramage

CERN, European Organization for Nuclear Research, Geneva, Switzerland

D. Abbaneo, J. Alimena, E. Auffray, G. Auzinger, J. Baechler, P. Baillon[†], D. Barney, J. Bendavid, M. Bianco, B. Bilin, A. Bocci, E. Brondolin, C. Caillol, T. Camporesi, G. Cerminara, N. Chernyavskaya, S.S. Chhibra, S. Choudhury, M. Cipriani, L. Cristella, D. d'Enterria, A. Dabrowski, A. David, A. De Roeck, M.M. Defranchis, M. Deile, M. Dobson, M. Dünser, N. Dupont, F. Fallavollita[59], A. Florent, L. Forthomme, G. Franzoni, W. Funk, S. Ghosh, S. Giani, D. Gigi, K. Gill, F. Glege, L. Gouskos, E. Govorkova, M. Haranko, J. Hegeman, V. Innocente, T. James, P. Janot, J. Kaspar, J. Kieseler, N. Kratochwil, S. Laurila, P. Lecoq, E. Leutgeb, A. Lintuluoto, C. Lourenço, B. Maier, L. Malgeri, M. Mannelli, A.C. Marini, F. Meijers, S. Mersi, E. Meschi, F. Moortgat, M. Mulders, S. Orfanelli, L. Orsini, F. Pantaleo, E. Perez, M. Peruzzi, A. Petrilli, G. Petrucciani, A. Pfeiffer, M. Pierini, D. Piparo, M. Pitt, H. Qu, T. Quast, D. Rabady, A. Racz, G. Reales Gutiérrez, M. Rovere, H. Sakulin, J. Salfeld-Nebgen, S. Scarfi, M. Selvaggi, A. Sharma, P. Silva, P. Sphicas[60], A.G. Stahl Leiton, S. Summers, K. Tatar, V.R. Tavolaro, D. Treille, P. Tropea, A. Tsirou, J. Wanczyk[61], K.A. Wozniak, W.D. Zeuner

Paul Scherrer Institut, Villigen, Switzerland

L. Caminada[62], A. Ebrahimi, W. Erdmann, R. Horisberger, Q. Ingram, H.C. Kaestli, D. Kotlinski, C. Lange, M. Missiroli[62], L. Noehte[62], T. Rohe

ETH Zurich - Institute for Particle Physics and Astrophysics (IPA), Zurich, Switzerland

T.K. Aarrestad, K. Androsov[61], M. Backhaus, P. Berger, A. Calandri, K. Datta, A. De Cosa, G. Dissertori, M. Dittmar, M. Donegà, F. Eble, M. Galli, K. Gedia, F. Glessgen, T.A. Gómez Espinosa, C. Grab, D. Hits, W. Lustermann, A.-M. Lyon, R.A. Manzoni, L. Marchese, C. Martin Perez, A. Mascellani[61], F. Nessi-Tedaldi, J. Niedziela, F. Pauss, V. Perovic, S. Pigazzini, M.G. Ratti, M. Reichmann, C. Reissel, T. Reitenspiess, B. Ristic, F. Riti, D. Ruini, D.A. Sanz Becerra, J. Steggemann[61], D. Valsecchi[27], R. Wallny

Universität Zürich, Zurich, Switzerland

C. Amsler[63], P. Bärtschi, C. Botta, D. Brzhechko, M.F. Canelli, K. Cormier, A. De Wit, R. Del Burgo, J.K. Heikkilä, M. Huwiler, W. Jin, A. Jofrehei,

B. Kilminster, S. Leontsinis, S.P. Liechti, A. Macchiolo, P. Meiring, V.M. Mikuni, U. Molinatti, I. Neutelings, A. Reimers, P. Robmann, S. Sanchez Cruz, K. Schweiger, M. Senger, Y. Takahashi

National Central University, Chung-Li, Taiwan
C. Adloff[64], C.M. Kuo, W. Lin, P.K. Rout, S.S. Yu

National Taiwan University (NTU), Taipei, Taiwan
L. Ceard, Y. Chao, K.F. Chen, P.s. Chen, H. Cheng, W.-S. Hou, R. Khurana, G. Kole, Y.y. Li, R.-S. Lu, E. Paganis, A. Psallidas, A. Steen, H.y. Wu, E. Yazgan, P.r. Yu

Chulalongkorn University, Faculty of Science, Department of Physics, Bangkok, Thailand
C. Asawatangtrakuldee, N. Srimanobhas

Çukurova University, Physics Department, Science and Art Faculty, Adana, Turkey
D. Agyel, F. Boran, Z.S. Demiroglu, F. Dolek, I. Dumanoglu[65], E. Eskut, Y. Guler[66], E. Gurpinar Guler[66], C. Isik, O. Kara, A. Kayis Topaksu, U. Kiminsu, G. Onengut, K. Ozdemir[67], A. Polatoz, A.E. Simsek, B. Tali[68], U.G. Tok, S. Turkcapar, E. Uslan, I.S. Zorbakir

Middle East Technical University, Physics Department, Ankara, Turkey
G. Karapinar[69], K. Ocalan[70], M. Yalvac[71]

Bogazici University, Istanbul, Turkey
B. Akgun, I.O. Atakisi, E. Gülmez, M. Kaya[72], O. Kaya[73], S. Tekten[74]

Istanbul Technical University, Istanbul, Turkey
A. Cakir, K. Cankocak[65], Y. Komurcu, S. Sen[65]

Istanbul University, Istanbul, Turkey
O. Aydilek, S. Cerci[68], B. Hacisahinoglu, I. Hos[75], B. Isildak[76], B. Kaynak, S. Ozkorucuklu, C. Simsek, D. Sunar Cerci[68]

Institute for Scintillation Materials of National Academy of Science of Ukraine, Kharkiv, Ukraine
B. Grynyov

National Science Centre, Kharkiv Institute of Physics and Technology, Kharkiv, Ukraine
L. Levchuk

University of Bristol, Bristol, United Kingdom
D. Anthony, E. Bhal, J.J. Brooke, A. Bundock, E. Clement, D. Cussans, H. Flacher, M. Glowacki, J. Goldstein, G.P. Heath, H.F. Heath, L. Kreczko,

JHEP07(2023)046

B. Krikler, S. Paramesvaran, S. Seif El Nasr-Storey, V.J. Smith, N. Stylianou[77], K. Walkingshaw Pass, R. White

Rutherford Appleton Laboratory, Didcot, United Kingdom
A.H. Ball, K.W. Bell, A. Belyaev[78], C. Brew, R.M. Brown, D.J.A. Cockerill, C. Cooke, K.V. Ellis, K. Harder, S. Harper, M.-L. Holmberg[79], J. Linacre, K. Manolopoulos, D.M. Newbold, E. Olaiya, D. Petyt, T. Reis, G. Salvi, T. Schuh, C.H. Shepherd-Themistocleous, I.R. Tomalin, T. Williams

Imperial College, London, United Kingdom
R. Bainbridge, P. Bloch, S. Bonomally, J. Borg, S. Breeze, C.E. Brown, O. Buchmuller, V. Cacchio, V. Cepaitis, G.S. Chahal[80], D. Colling, J.S. Dancu, P. Dauncey, G. Davies, J. Davies, M. Della Negra, S. Fayer, G. Fedi, G. Hall, M.H. Hassanshahi, A. Howard, G. Iles, J. Langford, L. Lyons, A.-M. Magnan, S. Malik, A. Martelli, M. Mieskolainen, D.G. Monk, J. Nash[81], M. Pesaresi, B.C. Radburn-Smith, D.M. Raymond, A. Richards, A. Rose, E. Scott, C. Seez, A. Shtipliyski, R. Shukla, A. Tapper, K. Uchida, G.P. Uttley, L.H. Vage, T. Virdee[27], M. Vojinovic, N. Wardle, S.N. Webb, D. Winterbottom

Brunel University, Uxbridge, United Kingdom
K. Coldham, J.E. Cole, A. Khan, P. Kyberd, I.D. Reid

Baylor University, Waco, Texas, USA
S. Abdullin, A. Brinkerhoff, B. Caraway, J. Dittmann, K. Hatakeyama, A.R. Kanuganti, B. McMaster, M. Saunders, S. Sawant, C. Sutantawibul, J. Wilson

Catholic University of America, Washington, DC, USA
R. Bartek, A. Dominguez, R. Uniyal, A.M. Vargas Hernandez

The University of Alabama, Tuscaloosa, Alabama, USA
S.I. Cooper, D. Di Croce, S.V. Gleyzer, C. Henderson, C.U. Perez, P. Rumerio[82], C. West

Boston University, Boston, Massachusetts, USA
A. Akpinar, A. Albert, D. Arcaro, C. Cosby, Z. Demiragli, C. Erice, E. Fontanesi, D. Gastler, S. May, J. Rohlf, K. Salyer, D. Sperka, D. Spitzbart, I. Suarez, A. Tsatsos, S. Yuan

Brown University, Providence, Rhode Island, USA
G. Benelli, B. Burkle, X. Coubez[22], D. Cutts, M. Hadley, U. Heintz, J.M. Hogan[83], T. Kwon, G. Landsberg, K.T. Lau, D. Li, J. Luo, M. Narain, N. Pervan, S. Sagir[84], F. Simpson, E. Usai, W.Y. Wong, X. Yan, D. Yu, W. Zhang

University of California, Davis, Davis, California, USA
J. Bonilla, C. Brainerd, R. Breedon, M. Calderon De La Barca Sanchez, M. Chertok, J. Conway, P.T. Cox, R. Erbacher, G. Haza, F. Jensen, O. Kukral, G. Mocellin, M. Mulhearn, D. Pellett, B. Regnery, Y. Yao, F. Zhang

JHEP07(2023)046

University of California, Los Angeles, California, USA
M. Bachtis, R. Cousins, A. Datta, D. Hamilton, J. Hauser, M. Ignatenko, M.A. Iqbal, T. Lam, E. Manca, W.A. Nash, S. Regnard, D. Saltzberg, B. Stone, V. Valuev

University of California, Riverside, Riverside, California, USA
R. Clare, J.W. Gary, M. Gordon, G. Hanson, G. Karapostoli, O.R. Long, N. Manganelli, W. Si, S. Wimpenny

University of California, San Diego, La Jolla, California, USA
J.G. Branson, P. Chang, S. Cittolin, S. Cooperstein, D. Diaz, J. Duarte, R. Gerosa, L. Giannini, J. Guiang, R. Kansal, V. Krutelyov, R. Lee, J. Letts, M. Masciovecchio, F. Mokhtar, M. Pieri, B.V. Sathia Narayanan, V. Sharma, M. Tadel, E. Vourliotis, F. Würthwein, Y. Xiang, A. Yagil

University of California, Santa Barbara - Department of Physics, Santa Barbara, California, USA
N. Amin, C. Campagnari, M. Citron, G. Collura, A. Dorsett, V. Dutta, J. Incandela, M. Kilpatrick, J. Kim, A.J. Li, P. Masterson, H. Mei, M. Oshiro, M. Quinnan, J. Richman, U. Sarica, R. Schmitz, F. Setti, J. Sheplock, P. Siddireddy, D. Stuart, S. Wang

California Institute of Technology, Pasadena, California, USA
A. Bornheim, O. Cerri, I. Dutta, A. Latorre, J.M. Lawhorn, N. Lu, J. Mao, H.B. Newman, T. Q. Nguyen, M. Spiropulu, J.R. Vlimant, C. Wang, S. Xie, R.Y. Zhu

Carnegie Mellon University, Pittsburgh, Pennsylvania, USA
J. Alison, S. An, M.B. Andrews, P. Bryant, T. Ferguson, A. Harilal, C. Liu, T. Mudholkar, S. Murthy, M. Paulini, A. Roberts, A. Sanchez, W. Terrill

University of Colorado Boulder, Boulder, Colorado, USA
J.P. Cumalat, W.T. Ford, A. Hassani, G. Karathanasis, E. MacDonald, F. Marini, R. Patel, A. Perloff, C. Savard, N. Schonbeck, K. Stenson, K.A. Ulmer, S.R. Wagner, N. Zipper

Cornell University, Ithaca, New York, USA
J. Alexander, S. Bright-Thonney, X. Chen, D.J. Cranshaw, J. Fan, X. Fan, D. Gadkari, S. Hogan, J. Monroy, J.R. Patterson, D. Quach, J. Reichert, M. Reid, A. Ryd, J. Thom, P. Wittich, R. Zou

Fermi National Accelerator Laboratory, Batavia, Illinois, USA
M. Albrow, M. Alyari, G. Apollinari, A. Apresyan, L.A.T. Bauerdick, D. Berry, J. Berryhill, P.C. Bhat, K. Burkett, J.N. Butler, A. Canepa, G.B. Cerati, H.W.K. Cheung, F. Chlebana, K.F. Di Petrillo, J. Dickinson, V.D. Elvira, Y. Feng,

JHEP07(2023)046

J. Freeman, A. Gandrakota, Z. Gecse, L. Gray, D. Green, S. Grünendahl, O. Gutsche, R.M. Harris, R. Heller, T.C. Herwig, J. Hirschauer, L. Horyn, B. Jayatilaka, S. Jindariani, M. Johnson, U. Joshi, T. Klijnsma, B. Klima, K.H.M. Kwok, S. Lammel, D. Lincoln, R. Lipton, T. Liu, C. Madrid, K. Maeshima, C. Mantilla, D. Mason, P. McBride, P. Merkel, S. Mrenna, S. Nahn, J. Ngadiuba, D. Noonan, V. Papadimitriou, N. Pastika, K. Pedro, C. Pena[85], F. Ravera, A. Reinsvold Hall[86], L. Ristori, E. Sexton-Kennedy, N. Smith, A. Soha, L. Spiegel, J. Strait, L. Taylor, S. Tkaczyk, N.V. Tran, L. Uplegger, E.W. Vaandering, H.A. Weber, I. Zoi

University of Florida, Gainesville, Florida, USA

P. Avery, D. Bourilkov, L. Cadamuro, V. Cherepanov, R.D. Field, D. Guerrero, M. Kim, E. Koenig, J. Konigsberg, A. Korytov, K.H. Lo, K. Matchev, N. Menendez, G. Mitselmakher, A. Muthirakalayil Madhu, N. Rawal, D. Rosenzweig, S. Rosenzweig, K. Shi, J. Wang, Z. Wu

Florida State University, Tallahassee, Florida, USA

T. Adams, A. Askew, R. Habibullah, V. Hagopian, T. Kolberg, G. Martinez, H. Prosper, C. Schiber, O. Viazlo, R. Yohay, J. Zhang

Florida Institute of Technology, Melbourne, Florida, USA

M.M. Baarmand, S. Butalla, T. Elkafrawy[52], M. Hohlmann, R. Kumar Verma, M. Rahmani, F. Yumiceva

University of Illinois at Chicago (UIC), Chicago, Illinois, USA

M.R. Adams, H. Becerril Gonzalez, R. Cavanaugh, S. Dittmer, O. Evdokimov, C.E. Gerber, D.J. Hofman, D. S. Lemos, A.H. Merrit, C. Mills, G. Oh, T. Roy, S. Rudrabhatla, M.B. Tonjes, N. Varelas, X. Wang, Z. Ye, J. Yoo

The University of Iowa, Iowa City, Iowa, USA

M. Alhusseini, K. Dilsiz[87], L. Emediato, R.P. Gandrajula, G. Karaman, O.K. Köseyan, J.-P. Merlo, A. Mestvirishvili[88], J. Nachtman, O. Neogi, H. Ogul[89], Y. Onel, A. Penzo, C. Snyder, E. Tiras[90]

Johns Hopkins University, Baltimore, Maryland, USA

O. Amram, B. Blumenfeld, L. Corcodilos, J. Davis, A.V. Gritsan, S. Kyriacou, P. Maksimovic, J. Roskes, S. Sekhar, M. Swartz, T.Á. Vámi

The University of Kansas, Lawrence, Kansas, USA

A. Abreu, L.F. Alcerro Alcerro, J. Anguiano, P. Baringer, A. Bean, Z. Flowers, T. Isidori, J. King, G. Krintiras, M. Lazarovits, C. Le Mahieu, C. Lindsey, J. Marquez, N. Minafra, M. Murray, M. Nickel, C. Rogan, C. Royon, R. Salvatico, S. Sanders, C. Smith, Q. Wang, J. Williams, G. Wilson

Kansas State University, Manhattan, Kansas, USA

B. Allmond, S. Duric, A. Ivanov, K. Kaadze, D. Kim, Y. Maravin, T. Mitchell, A. Modak, K. Nam, D. Roy

JHEP07(2023)046

Lawrence Livermore National Laboratory, Livermore, California, USA
F. Rebassoo, D. Wright

University of Maryland, College Park, Maryland, USA
E. Adams, A. Baden, O. Baron, A. Belloni, A. Bethani, S.C. Eno, N.J. Hadley, S. Jabeen, R.G. Kellogg, T. Koeth, Y. Lai, S. Lascio, A.C. Mignerey, S. Nabili, C. Palmer, C. Papageorgakis, L. Wang, K. Wong

Massachusetts Institute of Technology, Cambridge, Massachusetts, USA
D. Abercrombie, W. Busza, I.A. Cali, Y. Chen, M. D'Alfonso, J. Eysermans, C. Freer, G. Gomez-Ceballos, M. Goncharov, P. Harris, M. Hu, D. Kovalskyi, J. Krupa, Y.-J. Lee, K. Long, C. Mironov, C. Paus, D. Rankin, C. Roland, G. Roland, Z. Shi, G.S.F. Stephans, J. Wang, Z. Wang, B. Wyslouch, T. J. Yang

University of Minnesota, Minneapolis, Minnesota, USA
R.M. Chatterjee, B. Crossman, A. Evans, J. Hiltbrand, Sh. Jain, B.M. Joshi, C. Kapsiak, M. Krohn, Y. Kubota, J. Mans, M. Revering, R. Rusack, R. Saradhy, N. Schroeder, N. Strobbe, M.A. Wadud

University of Mississippi, Oxford, Mississippi, USA
L.M. Cremaldi

University of Nebraska-Lincoln, Lincoln, Nebraska, USA
K. Bloom, M. Bryson, D.R. Claes, C. Fangmeier, L. Finco, F. Golf, C. Joo, R. Kamalieddin, I. Kravchenko, I. Reed, J.E. Siado, G.R. Snow[†], W. Tabb, A. Wightman, F. Yan, A.G. Zecchinelli

State University of New York at Buffalo, Buffalo, New York, USA
G. Agarwal, H. Bandyopadhyay, L. Hay, I. Iashvili, A. Kharchilava, C. McLean, M. Morris, D. Nguyen, J. Pekkanen, S. Rappoccio, A. Williams

Northeastern University, Boston, Massachusetts, USA
G. Alverson, E. Barberis, Y. Haddad, Y. Han, A. Krishna, J. Li, J. Lidrych, G. Madigan, B. Marzocchi, D.M. Morse, V. Nguyen, T. Orimoto, A. Parker, L. Skinnari, A. Tishelman-Charny, T. Wamorkar, B. Wang, A. Wisecarver, D. Wood

Northwestern University, Evanston, Illinois, USA
S. Bhattacharya, J. Bueghly, Z. Chen, A. Gilbert, K.A. Hahn, Y. Liu, N. Odell, M.H. Schmitt, M. Velasco

University of Notre Dame, Notre Dame, Indiana, USA
R. Band, R. Bucci, M. Cremonesi, A. Das, R. Goldouzian, M. Hildreth, K. Hurtado Anampa, C. Jessop, K. Lannon, J. Lawrence, N. Loukas, L. Lutton, J. Mariano, N. Marinelli, I. Mcalister, T. McCauley, C. Mcgrady, K. Mohrman,

JHEP07(2023)046

C. Moore, Y. Musienko[13], R. Ruchti, A. Townsend, M. Wayne, H. Yockey, M. Zarucki, L. Zygala

The Ohio State University, Columbus, Ohio, USA
B. Bylsma, M. Carrigan, L.S. Durkin, B. Francis, C. Hill, M. Joyce, A. Lesauvage, M. Nunez Ornelas, K. Wei, B.L. Winer, B. R. Yates

Princeton University, Princeton, New Jersey, USA
F.M. Addesa, P. Das, G. Dezoort, P. Elmer, A. Frankenthal, B. Greenberg, N. Haubrich, S. Higginbotham, A. Kalogeropoulos, G. Kopp, S. Kwan, D. Lange, D. Marlow, K. Mei, I. Ojalvo, J. Olsen, D. Stickland, C. Tully

University of Puerto Rico, Mayaguez, Puerto Rico, USA
S. Malik, S. Norberg

Purdue University, West Lafayette, Indiana, USA
A.S. Bakshi, V.E. Barnes, R. Chawla, S. Das, L. Gutay, M. Jones, A.W. Jung, D. Kondratyev, A.M. Koshy, M. Liu, G. Negro, N. Neumeister, G. Paspalaki, S. Piperov, A. Purohit, J.F. Schulte, M. Stojanovic, J. Thieman, F. Wang, R. Xiao, W. Xie

Purdue University Northwest, Hammond, Indiana, USA
J. Dolen, N. Parashar

Rice University, Houston, Texas, USA
D. Acosta, A. Baty, T. Carnahan, M. Decaro, S. Dildick, K.M. Ecklund, P.J. Fernández Manteca, S. Freed, P. Gardner, F.J.M. Geurts, A. Kumar, W. Li, B.P. Padley, R. Redjimi, J. Rotter, W. Shi, S. Yang, E. Yigitbasi, L. Zhang[91], Y. Zhang

University of Rochester, Rochester, New York, USA
A. Bodek, P. de Barbaro, R. Demina, J.L. Dulemba, C. Fallon, T. Ferbel, M. Galanti, A. Garcia-Bellido, O. Hindrichs, A. Khukhunaishvili, E. Ranken, R. Taus, G.P. Van Onsem

The Rockefeller University, New York, New York, USA
K. Goulianos

Rutgers, The State University of New Jersey, Piscataway, New Jersey, USA
B. Chiarito, J.P. Chou, Y. Gershtein, E. Halkiadakis, A. Hart, M. Heindl, D. Jaroslawski, O. Karacheban[25], I. Laflotte, A. Lath, R. Montalvo, K. Nash, M. Osherson, H. Routray, S. Salur, S. Schnetzer, S. Somalwar, R. Stone, S.A. Thayil, S. Thomas, H. Wang

University of Tennessee, Knoxville, Tennessee, USA
H. Acharya, A.G. Delannoy, S. Fiorendi, T. Holmes, E. Nibigira, S. Spanier

JHEP07(2023)046

Texas A&M University, College Station, Texas, USA
O. Bouhali[92], M. Dalchenko, A. Delgado, R. Eusebi, J. Gilmore, T. Huang, T. Kamon[93], H. Kim, S. Luo, S. Malhotra, R. Mueller, D. Overton, D. Rathjens, A. Safonov

Texas Tech University, Lubbock, Texas, USA
N. Akchurin, J. Damgov, V. Hegde, K. Lamichhane, S.W. Lee, T. Mengke, S. Muthumuni, T. Peltola, I. Volobouev, A. Whitbeck

Vanderbilt University, Nashville, Tennessee, USA
E. Appelt, S. Greene, A. Gurrola, W. Johns, A. Melo, F. Romeo, P. Sheldon, S. Tuo, J. Velkovska, J. Viinikainen

University of Virginia, Charlottesville, Virginia, USA
B. Cardwell, B. Cox, G. Cummings, J. Hakala, R. Hirosky, A. Ledovskoy, A. Li, C. Neu, C.E. Perez Lara, B. Tannenwald

Wayne State University, Detroit, Michigan, USA
P.E. Karchin, N. Poudyal

University of Wisconsin — Madison, Madison, Wisconsin, USA
S. Banerjee, K. Black, T. Bose, S. Dasu, I. De Bruyn, P. Everaerts, C. Galloni, H. He, M. Herndon, A. Herve, C.K. Koraka, A. Lanaro, A. Loeliger, R. Loveless, J. Madhusudanan Sreekala, A. Mallampalli, A. Mohammadi, S. Mondal, G. Parida, D. Pinna, A. Savin, V. Shang, V. Sharma, W.H. Smith, D. Teague, H.F. Tsoi, W. Vetens

Authors affiliated with an institute or an international laboratory covered by a cooperation agreement with CERN
†: Deceased
S. Afanasiev, V. Andreev, Yu. Andreev, T. Aushev, M. Azarkin, A. Babaev, A. Belyaev, V. Blinov[94], E. Boos, V. Borshch, D. Budkouski, V. Bunichev, V. Chekhovsky, R. Chistov[94], A. Dermenev, T. Dimova[94], I. Dremin, M. Dubinin[85], L. Dudko, V. Epshteyn, A. Ershov, G. Gavrilov, V. Gavrilov, S. Gninenko, V. Golovtcov, N. Golubev, I. Golutvin, I. Gorbunov, A. Gribushin, V. Ivanchenko, Y. Ivanov, V. Kachanov, L. Kardapoltsev[94], V. Karjavine, A. Karneyeu, V. Kim[94], M. Kirakosyan, D. Kirpichnikov, M. Kirsanov, V. Klyukhin, D. Konstantinov, V. Korenkov, A. Kozyrev[94], N. Krasnikov, E. Kuznetsova[95], A. Lanev, P. Levchenko, A. Litomin, N. Lychkovskaya, V. Makarenko, A. Malakhov, V. Matveev[94], V. Murzin, A. Nikitenko[96], S. Obraztsov, A. Oskin, I. Ovtin[94], V. Palichik, P. Parygin, V. Perelygin, M. Perfilov, S. Polikarpov[94], V. Popov, E. Popova, O. Radchenko[94], M. Savina, V. Savrin, D. Selivanova, V. Shalaev, S. Shmatov, S. Shulha, Y. Skovpen[94], S. Slabospitskii, V. Smirnov, D. Sosnov, V. Sulimov, E. Tcherniaev, A. Terkulov, O. Teryaev, I. Tlisova, M. Toms, A. Toropin, L. Uvarov, A. Uzunian,

E. Vlasov, P. Volkov, A. Vorobyev, N. Voytishin, B.S. Yuldashev[97], A. Zarubin, I. Zhizhin, A. Zhokin

[1] Also at Yerevan State University, Yerevan, Armenia
[2] Also at TU Wien, Vienna, Austria
[3] Also at Institute of Basic and Applied Sciences, Faculty of Engineering, Arab Academy for Science, Technology and Maritime Transport, Alexandria, Egypt
[4] Also at Université Libre de Bruxelles, Bruxelles, Belgium
[5] Also at Universidade Estadual de Campinas, Campinas, Brazil
[6] Also at Federal University of Rio Grande do Sul, Porto Alegre, Brazil
[7] Also at UFMS, Nova Andradina, Brazil
[8] Also at The University of the State of Amazonas, Manaus, Brazil
[9] Also at University of Chinese Academy of Sciences, Beijing, China
[10] Also at Nanjing Normal University Department of Physics, Nanjing, China
[11] Now at The University of Iowa, Iowa City, Iowa, USA
[12] Also at University of Chinese Academy of Sciences, Beijing, China
[13] Also at an institute or an international laboratory covered by a cooperation agreement with CERN
[14] Also at Cairo University, Cairo, Egypt
[15] Also at Suez University, Suez, Egypt
[16] Now at British University in Egypt, Cairo, Egypt
[17] Also at Purdue University, West Lafayette, Indiana, USA
[18] Also at Université de Haute Alsace, Mulhouse, France
[19] Also at Department of Physics, Tsinghua University, Beijing, China
[20] Also at Erzincan Binali Yildirim University, Erzincan, Turkey
[21] Also at University of Hamburg, Hamburg, Germany
[22] Also at RWTH Aachen University, III. Physikalisches Institut A, Aachen, Germany
[23] Also at Isfahan University of Technology, Isfahan, Iran
[24] Also at Bergische University Wuppertal (BUW), Wuppertal, Germany
[25] Also at Brandenburg University of Technology, Cottbus, Germany
[26] Also at Forschungszentrum Jülich, Juelich, Germany
[27] Also at CERN, European Organization for Nuclear Research, Geneva, Switzerland
[28] Also at Physics Department, Faculty of Science, Assiut University, Assiut, Egypt
[29] Also at Karoly Robert Campus, MATE Institute of Technology, Gyongyos, Hungary
[30] Also at Wigner Research Centre for Physics, Budapest, Hungary
[31] Also at Institute of Physics, University of Debrecen, Debrecen, Hungary
[32] Also at Institute of Nuclear Research ATOMKI, Debrecen, Hungary
[33] Now at Universitatea Babes-Bolyai — Facultatea de Fizica, Cluj-Napoca, Romania
[34] Also at Faculty of Informatics, University of Debrecen, Debrecen, Hungary
[35] Also at Punjab Agricultural University, Ludhiana, India
[36] Also at UPES — University of Petroleum and Energy Studies, Dehradun, India
[37] Also at University of Visva-Bharati, Santiniketan, India
[38] Also at University of Hyderabad, Hyderabad, India
[39] Also at Indian Institute of Science (IISc), Bangalore, India
[40] Also at Indian Institute of Technology (IIT), Mumbai, India
[41] Also at IIT Bhubaneswar, Bhubaneswar, India
[42] Also at Institute of Physics, Bhubaneswar, India
[43] Also at Deutsches Elektronen-Synchrotron, Hamburg, Germany
[44] Also at Sharif University of Technology, Tehran, Iran
[45] Also at Department of Physics, University of Science and Technology of Mazandaran, Behshahr, Iran
[46] Also at Helwan University, Cairo, Egypt
[47] Also at Italian National Agency for New Technologies, Energy and Sustainable Economic Development, Bologna, Italy
[48] Also at Centro Siciliano di Fisica Nucleare e di Struttura Della Materia, Catania, Italy

JHEP07(2023)046

[49] Also at Scuola Superiore Meridionale, Università di Napoli 'Federico II', Napoli, Italy
[50] Also at Fermi National Accelerator Laboratory, Batavia, Illinois, USA
[51] Also at Università di Napoli 'Federico II', Napoli, Italy
[52] Also at Ain Shams University, Cairo, Egypt
[53] Also at Consiglio Nazionale delle Ricerche — Istituto Officina dei Materiali, Perugia, Italy
[54] Also at Department of Applied Physics, Faculty of Science and Technology, Universiti Kebangsaan Malaysia, Bangi, Malaysia
[55] Also at Consejo Nacional de Ciencia y Tecnología, Mexico City, Mexico
[56] Also at IRFU, CEA, Université Paris-Saclay, Gif-sur-Yvette, France
[57] Also at Faculty of Physics, University of Belgrade, Belgrade, Serbia
[58] Also at Trincomalee Campus, Eastern University, Sri Lanka, Nilaveli, Sri Lanka
[59] Also at INFN Sezione di Pavia, Università di Pavia, Pavia, Italy
[60] Also at National and Kapodistrian University of Athens, Athens, Greece
[61] Also at Ecole Polytechnique Fédérale Lausanne, Lausanne, Switzerland
[62] Also at Universität Zürich, Zurich, Switzerland
[63] Also at Stefan Meyer Institute for Subatomic Physics, Vienna, Austria
[64] Also at Laboratoire d'Annecy-le-Vieux de Physique des Particules, IN2P3-CNRS, Annecy-le-Vieux, France
[65] Also at Near East University, Research Center of Experimental Health Science, Mersin, Turkey
[66] Also at Konya Technical University, Konya, Turkey
[67] Also at Izmir Bakircay University, Izmir, Turkey
[68] Also at Adiyaman University, Adiyaman, Turkey
[69] Also at Istanbul Gedik University, Istanbul, Turkey
[70] Also at Necmettin Erbakan University, Konya, Turkey
[71] Also at Bozok Universitetesi Rektörlügü, Yozgat, Turkey
[72] Also at Marmara University, Istanbul, Turkey
[73] Also at Milli Savunma University, Istanbul, Turkey
[74] Also at Kafkas University, Kars, Turkey
[75] Also at Istanbul University — Cerrahpasa, Faculty of Engineering, Istanbul, Turkey
[76] Also at Yildiz Technical University, Istanbul, Turkey
[77] Also at Vrije Universiteit Brussel, Brussel, Belgium
[78] Also at School of Physics and Astronomy, University of Southampton, Southampton, United Kingdom
[79] Also at University of Bristol, Bristol, United Kingdom
[80] Also at IPPP Durham University, Durham, United Kingdom
[81] Also at Monash University, Faculty of Science, Clayton, Australia
[82] Also at Università di Torino, Torino, Italy
[83] Also at Bethel University, St. Paul, Minnesota, USA
[84] Also at Karamanoğlu Mehmetbey University, Karaman, Turkey
[85] Also at California Institute of Technology, Pasadena, California, USA
[86] Also at United States Naval Academy, Annapolis, Maryland, USA
[87] Also at Bingol University, Bingol, Turkey
[88] Also at Georgian Technical University, Tbilisi, Georgia
[89] Also at Sinop University, Sinop, Turkey
[90] Also at Erciyes University, Kayseri, Turkey
[91] Also at Institute of Modern Physics and Key Laboratory of Nuclear Physics and Ion-beam Application (MOE) — Fudan University, Shanghai, China
[92] Also at Texas A&M University at Qatar, Doha, Qatar
[93] Also at Kyungpook National University, Daegu, Korea
[94] Also at another institute or international laboratory covered by a cooperation agreement with CERN
[95] Now at University of Florida, Gainesville, Florida, USA
[96] Also at Imperial College, London, United Kingdom
[97] Also at Institute of Nuclear Physics of the Uzbekistan Academy of Sciences, Tashkent, Uzbekistan

JHEP07(2023)046